USGS

science for a changing world

Techniques of Water-Resources Investigations
of the United States Geological Survey

Chapter A4

A MODULAR FINITE-ELEMENT MODEL (MODFE) FOR AREAL AND AXISYMMETRIC GROUND-WATER FLOW PROBLEMS, PART 2: DERIVATION OF FINITE-ELEMENT EQUATIONS AND COMPARISONS WITH ANALYTICAL SOLUTIONS

By Richard L. Cooley

Book 6
Chapter A4

Total water pumped into or out of wells $= \sum_{i=1}^{N} \sum_{e_i} \bar{P}^e_i \Delta t_{n+1} = \sum_{j=1}^{P} \bar{Q}_j \Delta t_{n+1}$.

Total water crossing specified-head boundaries $= \sum_{i=1}^{N} \bar{Q}_{Bi} \Delta t_{n+1}$.

Total water crossing Cauchy-type boundaries

$$= \frac{1}{2} \sum_{i=1}^{N} \sum_{j}' \left[\left(\bar{q}_B L \right)_{ij}' + \left(\alpha L \right)_{ij}' \left(\bar{H}_{Bi} - \bar{h}_i \right) \right] \Delta t_{n+1}.$$

Average volumetric flow rates in time element n+1 can be obtained by dividing the components by Δt_{n+1}, and running totals over time can be obtained by summing the components over all preceding time elements. The mass imbalance in time element n+1 is obtained by summing the components, and a running mass imbalance is obtained by summing mass imbalances over all preceding time elements.

EXTENSIONS OF THE BASIC EQUATIONS

Unconfined flow

When equation (1) is applied to areal flow in an unconfined aquifer by using the Dupuit approximation (Bear, 1979, p. 111-114), transmissivities are functions of the current saturated thickness of the aquifer, as follows:

$$\begin{aligned} T &= Kb \\ &= K\left(h - z_b \right), \end{aligned} \tag{65}$$

where b is the saturated thickness $h - z_b$ of the aquifer, h is the elevation of the water table above some datum, z_b is the elevation of the aquifer bottom referred to the same datum, and subscripts $\bar{x}$ and $\bar{y}$ were omitted from T and K for simplicity. Because b is head dependent and varies in time, equation (1) is nonlinear, with transmissivities that are head dependent and vary in time.

Time variance of the transmissivities can be handled in the same manner as time variance of B_i. That is, the G_{ij} coefficients, which contain the transmissivities, can be written for time element n+1 as

$$G_{ij} = G_{ij,n} \sigma_n + G_{ij,n+1} \sigma_{n+1}, \tag{66}$$

so that, by using the relationship $A_{ij} = G_{ij} + V_{ij}$, equation (54) is replaced with

$$\int_0^{\Delta t_{n+1}} A_{ij} \hat{h}_j \sigma_{n+1} dt'$$

26

$$= \int_0^{\Delta t_{n+1}} \left(G_{ij,n}\sigma_n + G_{ij,n+1}\sigma_{n+1} + V_{ij} \right) \left(\hat{h}_{j,n}\sigma_n + \hat{h}_{j,n+1}\sigma_{n+1} \right) \sigma_{n+1} dt'$$

$$= \frac{1}{12}\Delta t_{n+1} \left(G_{ij,n} + G_{ij,n+1} + 2V_{ij} \right) \hat{h}_{j,n}$$

$$+ \frac{1}{12}\Delta t_{n+1} \left(G_{ij,n} + 3G_{ij,n+1} + 4V_{ij} \right) \hat{h}_{j,n+1}. \tag{67}$$

For an aquifer that remains unconfined (that is, h never exceeds the elevation of the base of an overlying confining bed) throughout the simulation period, matrix $\underline{\underline{C}}$ is modified by replacing the storage coefficient, S^e, in each element by specific yield, S_y^e. Therefore, $\underline{\underline{C}}$ is constant in time. Conversions from confined to unconfined flow (and vice versa) and their effect on $\underline{\underline{C}}$ is discussed in a later section.

Use of equation (67) in place of equation (54) modifies equation (56) to

$$\underline{\underline{C}}\left(\hat{h}_{n+1} - \hat{h}_n \right) + \frac{1}{6}\Delta t_{n+1} \left(\underline{\underline{G}}_n + 3\underline{\underline{G}}_{n+1} + 4\underline{\underline{V}} \right) \hat{h}_{n+1}$$

$$+ \frac{1}{6}\Delta t_{n+1} \left(\underline{\underline{G}}_n + \underline{\underline{G}}_{n+1} + 2\underline{\underline{V}} \right) \hat{h}_n = \Delta t_{n+1}\bar{\underline{B}}, \tag{68}$$

where equation (61) was used for $\underline{B}$. Equation (68) can be written in a form analogous to equation (58) by using equation (57) and weighted average values of G_{ij}, defined as

$$\tilde{G}_{ij} = \frac{1}{4}\left(G_{ij,n} + 3G_{ij,n+1} \right) \tag{69}$$

and

$$\bar{G}_{ij} = \frac{1}{3}\left(G_{ij,n} + 2G_{ij,n+1} \right). \tag{70}$$

Thus,

$$\left[\frac{\underline{\underline{C}}}{(2/3)\Delta t_{n+1}} + \tilde{\underline{\underline{G}}} + \underline{\underline{V}} \right] \delta = \bar{\underline{B}} - \left(\bar{\underline{\underline{G}}} + \underline{\underline{V}} \right) \hat{h}_n. \tag{71}$$

Define the terms

$$d_{ij}^e = \frac{K_{xx}^e}{4\Delta^e} b_i^e b_j^e + \frac{K_{yy}^e}{4\Delta^e} c_i^e c_j^e, \quad i \neq j. \tag{72}$$

Then an off-diagonal element of $\underline{\underline{G}}$ is given by

$$G_{ij} = \sum_{e_i} \left(\frac{1}{3}\sum_s b_s \right) d_{ij}^e, \quad i \neq j, \tag{73}$$

27

where b_s is the aquifer thickness at node $s = k,l,m$, and $\frac{1}{3}\sum_s b_s$ is the average aquifer thickness in element e, assuming that thickness varies linearly over the element. Computation of G_{ij} using equation (73) requires reassembling G_{ij} element by element each time thickness b_s is changed. An approximation that Cooley (1971) found to be good for a subdomain finite-element solution of axisymmetric, variably saturated flow problems avoids this reassembly. The approximation is to evaluate the head-dependent coefficient in G_{ij} using the head half-way between nodes i and j. For the present problem, this approximation is equivalent to replacing $\frac{1}{3}\sum_s b_s$ in equation (73) with the average thickness between nodes i and j. Thus, the approximation is

$$G_{ij} \simeq \frac{1}{2}\left(b_i + b_j\right)\sum_{e_i} d_{ij}^e = \frac{1}{2}\left(b_i + b_j\right)D_{ij},\tag{74}$$

where

$$D_{ij} = \sum_{e_i} d_{ij}^e.\tag{75}$$

Because aquifer thickness is dependent upon head, a means of predicting this thickness at an advanced time level, n+1, is needed prior to solving equation (71). A simple and effective method is the predictor-corrector technique described by Douglas and Jones (1963). In the predictor step of this two-step process, the previously calculated thicknesses are used in $\underline{\underline{G}}$ to form an equation of the same form as equation (58). This equation is then solved for the head changes over the time element, and heads at the advanced time level are predicted based on equation (57). Aquifer thicknesses are then updated using the predicted head changes, and these updated thicknesses are used to form $\underline{\underline{\tilde{G}}}$ and $\underline{\underline{\bar{G}}}$. These matrices are used in equation (71) to solve for the head changes over the time element, which is the corrector step.

The predictor step is expressed by the following equations. Based on equation (58),

$$\left[\frac{\underline{\underline{C}}}{(2/3)\Delta t_{n+1}} + \underline{\underline{G}}_n + \underline{\underline{V}}\right]\underline{\delta}^* = \underline{\bar{B}} - \left(\underline{\underline{G}}_n + \underline{\underline{V}}\right)\underline{\hat{h}}_n\tag{76}$$

where $\underline{\delta}^*$ is the predicted head-change vector and

$$G_{ij,n} = \frac{1}{2}\left(b_{i,n} + b_{j,n}\right)D_{ij}, \quad i \neq j.\tag{77}$$

The thickness $b_{i,n}$ is

$$b_{i,n} = \hat{h}_{i,n} - z_{bi},\tag{78}$$

and $b_{j,n}$ is defined similarly. From equation (57), the predicted head vector, $\underline{\hat{h}}_n^*$, at time level t_{n+1} is

$$\hat{\underline{h}}^* = \frac{3}{2}\underline{\delta}^* + \hat{\underline{h}}_n. \tag{79}$$

The corrector step uses heads $\hat{\underline{h}}^*$ to form the following corrector equations. Based on equation (71)

$$\left[\frac{\underline{\underline{C}}}{(2/3)\Delta t_{n+1}} + \underline{\underline{\tilde{G}}}^* + \underline{\underline{V}}\right]\underline{\delta} = \bar{\underline{B}} - \left(\underline{\underline{\bar{G}}}^* + \underline{\underline{V}}\right)\hat{\underline{h}}_n, \tag{80}$$

where $\underline{\underline{\tilde{G}}}^*$ and $\underline{\underline{\bar{G}}}^*$ are the approximations of $\underline{\underline{\tilde{G}}}$ and $\underline{\underline{\bar{G}}}$, defined, using equations (69), (70), (74), and (79), as

$$\tilde{G}_{ij}^* = \frac{1}{4}\left\{\frac{1}{2}\left(b_{i,n} + b_{j,n}\right) + 3\left[\frac{1}{2}\left(b_{i,n} + \frac{3}{2}\delta_i^* + b_{j,n} + \frac{3}{2}\delta_j^*\right)\right]\right\}D_{ij}$$

$$= \frac{9}{16}\left[\delta_i^* + \delta_j^* + \frac{8}{9}\left(b_{i,n} + b_{j,n}\right)\right]D_{ij}, \quad i \neq j, \tag{81}$$

and

$$\bar{G}_{ij}^* = \frac{1}{3}\left\{\frac{1}{2}\left(b_{i,n} + b_{j,n}\right) + 2\left[\frac{1}{2}\left(b_{i,n} + \frac{3}{2}\delta_i^* + b_{j,n} + \frac{3}{2}\delta_j^*\right)\right]\right\}D_{ij}$$

$$= \frac{1}{2}\left(\delta_i^* + \delta_j^* + b_{i,n} + b_{j,n}\right)D_{ij}, \quad i \neq j. \tag{82}$$

In practice, to reduce round-off error $\left\{\underline{\underline{C}}/\left[(2/3)\Delta t_{n+1}\right] + \underline{\underline{\tilde{G}}}^* + \underline{\underline{V}}\right\}\underline{\delta}^*$ is subtracted from both sides of equation (80) to create a residual form of the equation so that $\underline{\delta} - \underline{\delta}^*$ is actually solved for. Head change $\underline{\delta}$ is then directly computed as $\underline{\delta} = \left(\underline{\delta} - \underline{\delta}^*\right) + \underline{\delta}^*$. The head at the end of the time element is calculated using equation (57).

Mass-balance calculations could be based on equation (80). However, more information about the accuracy of the predictor-corrector scheme can be obtained by computing mass-balance components from an equation derived from equation (71) in which $\underline{\underline{\tilde{G}}}$ and $\underline{\underline{\bar{G}}}$ are computed using $\hat{\underline{h}}_{n+1}$, which is

$$\frac{\underline{\underline{C}}}{(2/3)\Delta t_{n+1}}\underline{\delta} + \left(\underline{\underline{\tilde{G}}} + \underline{\underline{V}}\right)\underline{\delta} + \left(\underline{\underline{\bar{G}}} + \underline{\underline{V}}\right)\hat{\underline{h}}_n - \bar{\underline{B}}$$

$$- \frac{\underline{\underline{C}}}{(2/3)\Delta t_{n+1}}\underline{\delta} + \left(\underline{\underline{\bar{G}}} + \underline{\underline{V}}\right)\hat{\underline{h}} + \left(\underline{\underline{\tilde{G}}} - \underline{\underline{\bar{G}}}\right)\underline{\delta} - \bar{\underline{B}}$$

$$\approx \underline{0}, \tag{83}$$

29

where, by employing equations (57), (69), (70), and (74), it can be verified that

$$\widetilde{G}_{ij} - \bar{G}_{ij} = \frac{1}{16}\Big(\delta_i + \delta_j\Big)D_{ij}. \tag{84}$$

Equation (83) becomes equation (64) when $\underline{\underline{G}}$ is not time variant.

Because $\widetilde{\underline{\underline{G}}}$ and $\bar{\underline{\underline{G}}}$ are computed using $\hat{h}_{n+1}$ instead of $\hat{h}^*$, δ is only the approximate solution of equation (83). If the time element Δt_{n+1} is too large, then the approximate solution will be poor, and this will result in a large mass imbalance as computed using equation (83). In this case, the time-element size should be reduced.

The algorithm used to implement the predictor-corrector method is summarized by the following steps.

1. Predictor: Solve equation (76) for δ^*, and solve equation (79) for $\hat{\underline{h}}^*$. Then compute a predicted average head vector $\bar{h}^*$ using $\bar{h}^* = \delta^* + \hat{h}_n$.

2. Compute elements of $\widetilde{\underline{\underline{G}}}^*$ and $\bar{\underline{\underline{G}}}^*$ using equations (81) and (82).

3. Corrector: Solve the residual form of equation (80) for $\delta - \delta^*$, and compute the average head $\bar{h}$ using $\bar{h} = \delta - \delta^* + \bar{h}^*$, which is obtained by combining $\bar{h}^* = \delta^* + \hat{h}_n$ and $\bar{h} = \delta + \hat{h}_n$. Compute $\underline{\delta} = \Big(\underline{\delta} - \underline{\delta}^*\Big) + \underline{\delta}^*$.

4. Compute the weighted average mass-balance components using equation (83).

5. Update the aquifer thickness for the next time element using

$$\underline{b}_{n+1} = \frac{3}{2}\underline{\delta} + \underline{b}_n, \tag{85}$$

which is obtained by using the definition of b and equation (57).

6. Compute $\hat{h}_{n+1}$ using

$$\hat{\underline{h}}_{n+1} = \frac{1}{2}\underline{\delta} + \bar{\underline{h}}, \tag{86}$$

which is derived by combining equations (57) and (63).

7. Advance the time-element index, n, define a new Δt_{n+1}, and return to 1, unless the simulation time limit has been reached.

Drying and resaturation of nodes

If the water table declines to the base of the aquifer at a node during a simulation, then the node is said to "go dry" (figure 7). Although the aquifer thickness at the node is zero, horizontal flow to or from adjacent saturated nodes can still exist by virtue of equation (74). Thus, the node should remain active and hydraulic head at the node should still be calculated. An approximate method of simulating this process is to solve the finite-element equation (equation (71)) using zero aquifer thickness at dry nodes. Because the storage term C_{ii} is not altered when a node goes

dry, this use of equation (71) assumes (1) that water is released from or taken into storage in the aquifer where the saturated thickness is greater than zero and in the material underlying the aquifer where the saturated thickness is zero, (2) that the specific yield of the aquifer and underlying materials is the same, and (3) that both of these sources of water contribute to horizontal flow in the aquifer. If the material underlying the aquifer is explicitly incorporated into the simulation as a confining unit (R > 0), then this unit serves to vertically convey water to or from the aquifer in addition to releasing or taking on stored water at dry nodes. Because dry nodes are active nodes in the flow system, solution of equation (71) can produce heads that decline below the aquifer base so that the water table can move laterally away from the dry nodes (figure 7). In this case, the computed heads at the dry nodes can be thought of as effective heads that allow approximation of horizontal flow in the aquifer near the dry nodes. If all nodes j adjacent to a dry node i also are dry, then, from equation (74), all $G_{ij} = 0$, and horizontal flow in the aquifer near the dry node ceases. Water table decline at the dry node will also cease unless the underlying unit is a confining unit (R > 0) and $\hat{h}_i > H_i$, or the node is on a Cauchy-type boundary ($\alpha > 0$) and $\hat{h}_i > H_{Bi}$, or known sources and sinks in B_i are negative, which is treated below.

If a pumping well (or other specified sink) is located at a node that goes dry, then the net discharge at the node is too large for the aquifer to sustain. This incompatibility must be rectified by the investigator.
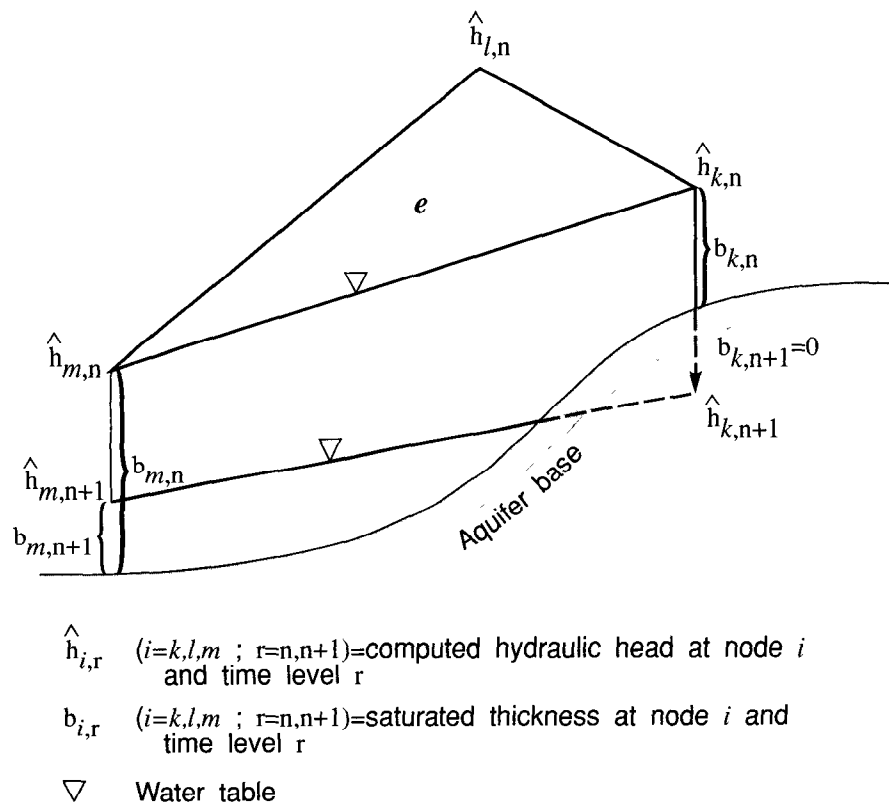

$\hat{h}_{i,r}$ ($i=k,l,m$; $r=n,n+1$)=computed hydraulic head at node i and time level r

$b_{i,r}$ ($i=k,l,m$; $r=n,n+1$)=saturated thickness at node i and time level r

$\triangledown$ Water table

Figure 7. Node k in element e drying up as the water table declines during simulation.

31

However, to allow the simulation to continue, and to suggest how much discharge the model can supply, the following automatic procedure is followed. If the net specified flux is negative at a node that is predicted to go dry at the end of a predictor step, then the net flux at the node is permanently cut in half beginning with the corrector step. Discharge can continue to be reduced by a factor of two on subsequent time elements if the node continues to go dry. If this procedure is insufficient to maintain a positive saturated thickness, the head at the node may drop below the aquifer base, and the dry node may at least temporarily supply water to the sink, which is physically unrealistic. However, the results of this procedure should indicate to the investigator how the model input could be changed to yield a physically compatible situation.

Combined confined and unconfined flow

Equation (1) can be applied to a problem where there is confined flow in some areas of the aquifer and unconfined flow in other areas. In this case, conversion can take place from one type of flow to another at any time or place in the aquifer (figure 8). Where flow is confined, the storage coefficient in equation (1) is the artesian storage coefficient, S, and transmissivity is constant in time. Where flow is unconfined, the storage coefficient is the specific yield, S_y, and transmissivity is time variant, as given by equation (65).

If flow at node i converts from confined to unconfined, or vice versa, during time-element $n+1$, the time interval Δt_{n+1} is divided into two subintervals, $\theta_i \Delta t_{n+1}$ and $(1-\theta_i)\Delta t_{n+1}$, where θ_i is the unknown proportionate point in the time interval when node i converts. The storage-change term analogous to equation (53) is then approximated as the sum of the two storage-change terms resulting from treating the two subintervals as subelements, each having its own basis functions and approximate function for hydraulic head. Thus, for the subinterval $\theta_i \Delta t_{n+1}$

where

$$\hat{h}_i = \hat{h}_{i,n}\sigma_n^{(1)} + z_{ti}\sigma_\theta^{(1)}, \qquad (87)$$

$$\sigma_n^{(1)} = 1 - \frac{\sigma_{n+1}}{\theta_i}, \qquad (88)$$

$$\sigma_\theta^{(1)} = \frac{\sigma_{n+1}}{\theta_i}, \qquad (89)$$

and z_{ti} is the elevation of the top of the aquifer and equals the head at node i at time $t_n + \theta_i \Delta t_{n+1}$. For the subinterval $\left(1-\theta_i\right)\Delta t_{n+1}$,

where

$$\hat{h}_i = z_{ti}\sigma_\theta^{(2)} + \hat{h}_{i,n+1}\sigma_{n+1}^{(2)}, \qquad (90)$$

$$\sigma_\theta^{(2)} = \frac{\sigma_n}{1-\theta_i}, \qquad (91)$$

$$\sigma_{n+1}^{(2)} = 1 - \frac{\sigma_n}{1-\theta_i}. \qquad (92)$$

32

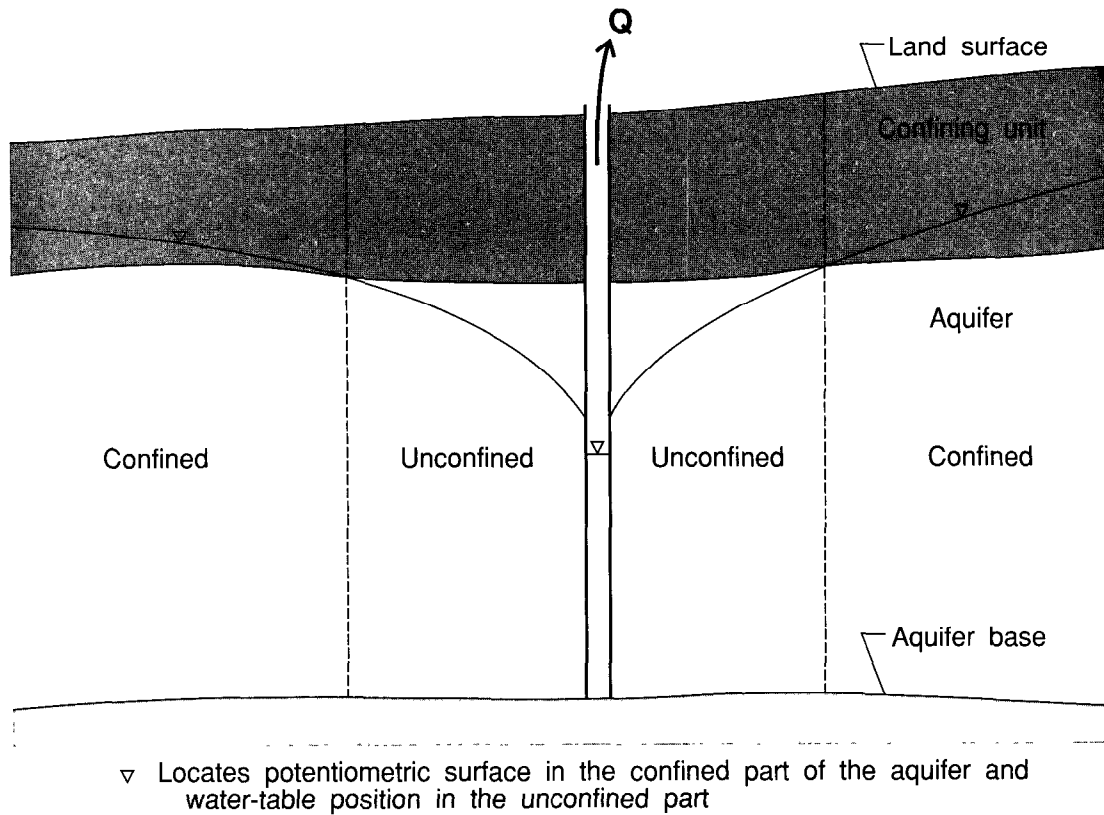▽ Locates potentiometric surface in the confined part of the aquifer and water-table position in the unconfined part

Figure 8. Cross section showing conversion from confined to unconfined flow at time t near a well pumped at volumetric rate Q.

By using equations (87) through (92), the integrals involving the storage term C_{ii} (see equation (53)) for both subintervals are formed and evaluated as

$$\int_0^{\theta_i \Delta t_{n+1}} C_{ii} \frac{d\hat{h}_i}{dt} \sigma_\theta^{(1)} dt' = C_{ii}^{(1)} \int_0^{\theta_i \Delta t_{n+1}} \left[\hat{h}_{i,n} \frac{d\sigma_n^{(1)}}{dt} + z_{ti} \frac{d\sigma_\theta^{(1)}}{dt} \right] \sigma_\theta^{(1)} dt'$$

$$= \frac{1}{2} C_{ii}^{(1)} \left[z_{ti} - \hat{h}_{i,n} \right] \tag{93}$$

and

$$\int_{\theta_i \Delta t_{n+1}}^{\Delta t_{n+1}} C_{ii} \frac{d\hat{h}_i}{dt} \sigma_{n+1}^{(2)} dt' = C_{ii}^{(2)} \int_{\theta_i \Delta t_{n+1}}^{\Delta t_{n+1}} \left[z_{ti} \frac{d\sigma_\theta^{(2)}}{dt} + \hat{h}_{i,n+1} \frac{d\sigma_{n+1}^{(2)}}{dt} \right] \sigma_{n+1}^{(2)} dt'$$

$$= \frac{1}{2} C_{ii}^{(2)} \left[\hat{h}_{i,n+1} - z_{ti} \right], \tag{94}$$

where $C_{ii}^{(1)}$ is the storage term before conversion, and $C_{ii}^{(2)}$ is the storage term after conversion.

33

The required finite-element equation for node i and time-element n+1 is obtained by summing the equations for the two subintervals, so that the storage-change term is the sum of equations (93) and (94). This sum is one-half the total change in water stored during time element n+1 (Prickett and Lonnquist, 1971, p. 40-41; Trescott and others, 1976, p. 10-11; and Wilson and others, 1979, p. 52). It is instructive to note that this sum can be written as

$$\frac{1}{2}C_{ii}^{(1)}\left(z_{ti} - \hat{h}_{i,n}\right) + \frac{1}{2}C_{ii}^{(2)}\left(\hat{h}_{i,n+1} - z_{ti}\right)$$

$$= \frac{1}{2}C_{ii}^{(1)}\left(z_{ti} - \hat{h}_{i,n}\right) + \frac{1}{2}C_{ii}^{(2)}\left(\hat{h}_{i,n+1} - \hat{h}_{i,n}\right) - \frac{1}{2}C_{ii}^{(2)}\left(z_{ti} - \hat{h}_{i,n}\right)$$

$$= \frac{1}{2}\left[C_{ii}^{(2)} + \left(C_{ii}^{(1)} - C_{ii}^{(2)}\right)\hat{\theta}_i\right]\left(\hat{h}_{i,n+1} - \hat{h}_{i,n}\right), \tag{95}$$

where

$$\hat{\theta}_i = \frac{z_{ti} - \hat{h}_{i,n}}{\hat{h}_{i,n+1} - \hat{h}_{i,n}}. \tag{96}$$

Therefore, if head is assumed to vary linearly within time-element n+1, $\hat{\theta}_i$ is an estimate of θ_i and the term in brackets defines an effective storage coefficient for time-element n+1.

By making use of equations (95) and (96) and approximating the sum of terms of the form of equation (67) for the two subintervals by the analogous term (equation 67) for the entire time element, an equation of the form of equation (68) may be written to include the possibility of one or more conversions within time-element n+1 as

$$\underline{\underline{C}}^{(2)}\left(\hat{\underline{h}}_{n+1} - \hat{\underline{h}}_n\right) + \left(\underline{\underline{C}}^{(1)} - \underline{\underline{C}}^{(2)}\right)\left(\underline{z}_t - \hat{\underline{h}}_n\right) + \frac{1}{6}\Delta t_{n+1}\left(\underline{\underline{G}}_n + 3\underline{\underline{G}}_{n+1} + 4\underline{\underline{V}}\right)\hat{\underline{h}}_{n+1}$$

$$+ \frac{1}{6}\Delta t_{n+1}\left(\underline{\underline{G}}_n + \underline{\underline{G}}_{n+1} + 2\underline{\underline{V}}\right)\hat{\underline{h}}_n = \Delta t_{n+1}\underline{\check{B}}, \tag{97}$$

where $C_{jj}^{(1)} = C_{jj}^{(2)}$ for all nodes that do not convert in the time interval Δt_{n+1}, and $\underline{z}_t$ is the vector of nodal aquifer-top elevations. Hence, the equation to replace equation (71) is

$$\left[\frac{\underline{\underline{C}}^{(2)}}{(2/3)\Delta t_{n+1}} + \tilde{\underline{\underline{G}}} + \underline{\underline{V}}\right]\underline{\delta} = \underline{\check{B}} - \left(\tilde{\underline{\underline{G}}} + \underline{\underline{V}}\right)\hat{\underline{h}}_n + \frac{\underline{\underline{C}}^{(2)} - \underline{\underline{C}}^{(1)}}{\Delta t_{n+1}}\left(\underline{z}_t - \hat{\underline{h}}_n\right). \tag{98}$$

The predictor-corrector method is used to solve equation (98). For the predictor step, the predicted head vector $\hat{\underline{h}}^*$ is obtained using equations (76) and (79) with $\underline{\underline{C}} = \underline{\underline{C}}^{(1)}$. These predicted heads are used to determine which nodes, if any, convert during the time interval and to estimate the saturated thickness for all nodes that are either unconfined during the entire time interval or convert from confined to unconfined conditions during the time interval.

Predicted heads $\hat{h}_i^*$ were found to be poor estimates of $\hat{h}_{i,n+1}$ for nodes that convert from confined to unconfined conditions; thus, they cannot be directly used to calculate saturated thickness for the corrector step. This problem occurs because the artesian storage coefficient is usually several orders of magnitude smaller than the specific yield, so that unless $\hat{\theta}_i \approx 1$,

34

the change from $c_{ii}^{(1)}$ to $c_{ii}^{(2)} + \left[c_{ii}^{(1)} - c_{ii}^{(2)}\right]\hat{\theta}_i$ is large. It was also found that total storage changes during confined to unconfined conversions are usually determined much more accurately in the predictor step than the head values. Therefore, an expression that can be used to revise a predicted head can be developed by equating the predicted change in storage, $c_{ii}^{(1)}\left(\hat{h}_i^* - \hat{h}_{i,n}\right)$, to the change in storage calculated with the conversion, to obtain

$$c_{ii}^{(1)}\left[z_{ti} - \hat{h}_{i,n}\right] + c_{ii}^{(2)}\left[\hat{h}_i' - z_{ti}\right] = c_{ii}^{(1)}\left[\hat{h}_i^* - \hat{h}_{i,n}\right], \qquad (99)$$

where $\hat{h}_i'$ is the revised predicted head. Solution of equation (99) for $\hat{h}_i'$ yields

$$\hat{h}_i' = \frac{c_{ii}^{(1)}}{c_{ii}^{(2)}}\left[\hat{h}_i^* - z_{ti}\right] + z_{ti}. \qquad (100)$$

For confined to unconfined conversions, $c_{ii}^{(1)} \ll c_{ii}^{(2)}$ so that $\hat{h}_{i,n} - \hat{h}_i'$ is much smaller than $\hat{h}_{i,n} - \hat{h}_i^*$. However, if $\hat{h}_i^*$ predicts a conversion, so will $\hat{h}_i'$.

The corrector step incorporates any possible conversions. If $\hat{h}_i^* < z_{ti} < \hat{h}_{i,n}$ or $\hat{h}_{i,n} < z_{ti} < \hat{h}_i^*$, then a conversion is assumed to have taken place. The corrector equation is

$$\left[\frac{\underline{\underline{C}}^{(2)}}{(2/3)\Delta t_{n+1}} + \underline{\underline{\tilde{G}}}^* + \underline{\underline{V}}\right]\underline{\delta} = \underline{B} - \left[\underline{\underline{\bar{G}}}^* + \underline{\underline{V}}\right]\underline{\hat{h}}_n + \frac{\underline{\underline{C}}^{(2)} - \underline{\underline{C}}^{(1)}}{\Delta t_{n+1}}\left[\underline{z}_t - \underline{\hat{h}}_n\right], \qquad (101)$$

where entries $\tilde{G}_{ij}^*$ and $\bar{G}_{ij}^*$ are computed using $\hat{h}_i^*$ or $\hat{h}_i'$ as appropriate.

As in the case of purely unconfined flow, the magnitudes of the errors generated by the predictor-corrector method are indicated by the mass-balance errors. If the errors are large, then the time element sizes should be reduced.

Point head-dependent discharge (springs and drainage wells)

The discharge rate from springs or drainage wells varies with the head in the aquifer and declines to zero as the head declines to some elevation z_p (figure 9). Discharge is zero as long as the head remains below z_p. Discharges from springs or drainage wells may be simulated by adding a point head-dependent sink function to equation (1) to give an equation of the form

$$\frac{\partial}{\partial x}\left(T_{xx}\frac{\partial h}{\partial x} + T_{xy}\frac{\partial h}{\partial y}\right) + \frac{\partial}{\partial y}\left(T_{yx}\frac{\partial h}{\partial x} + T_{yy}\frac{\partial h}{\partial y}\right)$$
$$+ R(H-h) + S_p + W + P = S\frac{\partial h}{\partial t}. \qquad (102)$$

The term S_p is the sink function, given by

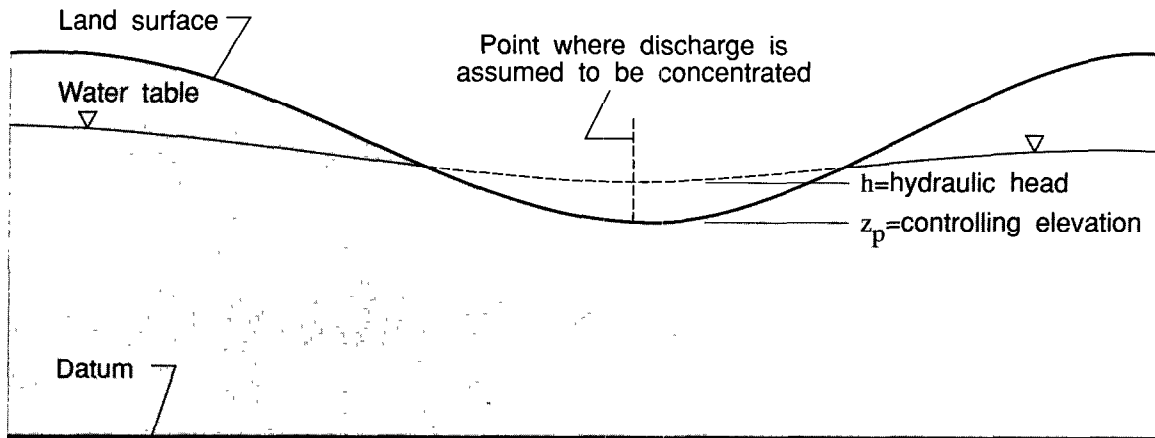$$S_p = \sum_{j=1}^{P_p}\delta\left(x - a_{pj}'\right)\delta\left(y - b_{pj}'\right)Q_{pj}, \qquad (103)$$

Figure 9. Cross section showing configuration of water-table position, ∇, and controlling elevation for point head-dependent discharge functions.

where Q_{pj} is the volumetric rate of head-dependent discharge [length^3/time] (negative for a sink) at point $\left(a'_{pj}, b'_{pj}\right)$, and there are P_p such points. Discharge Q_{pj} is assumed to vary linearly with head as long as head is greater than z_p. Thus, it is calculated from

$$Q_{pj} = \begin{cases} C_{pj}\left(z_p - h\right), & h > z_p \\ 0 & , h \le z_p \end{cases}, \tag{104}$$

where C_{pj} is a function of hydraulic conductance of aquifer materials in the vicinity of the spring or drainage well [length^2/time]. Nonlinearity of the sink function results from the fact that the form of the function is dependent on the head in the aquifer.

To incorporate equations (103) and (104) into the finite-element equations, it is assumed that the point sinks are located only at node points. Hence, spatial finite-element discretization is applied to equations (103) and (104) to yield
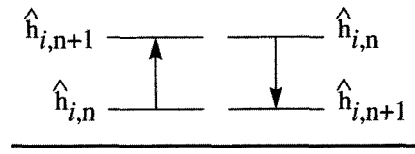
$$\sum_e \int_{\Delta_e} \int \bar{N}^e_i \sum_{j=1}^{P_p} \delta\left(\bar{x} - \bar{a}'_{pj}\right)\delta\left(\bar{y} - \bar{b}'_{pj}\right)Q_{pj}\,d\bar{x}d\bar{y}$$
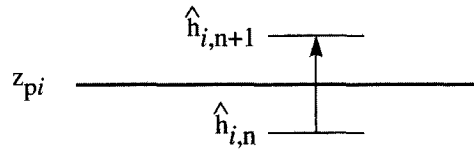
$$= Q_{pi} \tag{105}$$

where

$$Q_{pi} = \begin{cases} C_{pi}\left(z_{pi} - \hat{h}_i\right), & \hat{h}_i > z_{pi} \\ 0 & , \hat{h}_i \le z_{pi} \end{cases}, \tag{106}$$
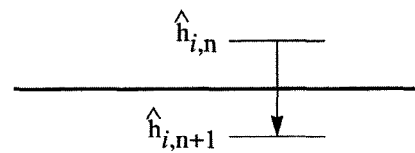
and subscript i indicates that the quantity is at node i.

36
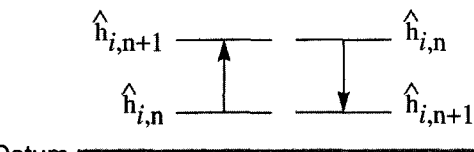
Case 1. Head above z_{pi} through-
out the time element

$\hat{h}_{i,n+1}$ ———— ———— $\hat{h}_{i,n}$

$\hat{h}_{i,n}$ ———— ———— $\hat{h}_{i,n+1}$

Case 3. Head rises above z_{pi}
within the time element

$\hat{h}_{i,n+1}$ ————

z_{pi}

$\hat{h}_{i,n}$ ————

———————— Datum ————————

Case 2. Head drops below z_{pi}
within the time element

$\hat{h}_{i,n}$ ————

z_{pi}

$\hat{h}_{i,n+1}$ ————

Case 4. Head below z_{pi} through-
out the time element

$\hat{h}_{i,n+1}$ ———— ———— $\hat{h}_{i,n}$

$\hat{h}_{i,n}$ ———— ———— $\hat{h}_{i,n+1}$

———————— Datum ————————

z_{pi} = controlling elevation at node i

$\hat{h}_{i,r}$ $(r=n,n+1)$ = hydraulic head at node i and at time level r

Figure 10. Four possible cases involving change in head over time element n+1 during which there is point head-dependent discharge.

To time integrate the sink function, four cases involving the change in head $\hat{h}_i$ over time element n+1 must be distinguished (figure 10). If the sink function changes form within the time element, then the element is divided into two subintervals, $\phi_i \Delta t_{n+1}$ and $\left(1 - \phi_i\right)\Delta t_{n+1}$, defined by proportional change-over point ϕ_i. Because head is assumed to vary linearly within the time element, ϕ_i is defined by

$$\phi_i = \frac{z_{pi} - \hat{h}_{i,n}}{\hat{h}_{i,n+1} - \hat{h}_{i,n}}. \tag{107}$$

Formulations for each of the four cases in figure 10 are as follows:

37

1. Head above z_{pi} throughout the time element.

$$\int_0^{\Delta t_{n+1}} C_{pi}\left(z_{pi} - \hat{h}_i\right)\sigma_{n+1}dt' = \int_0^{\Delta t_{n+1}} C_{pi}\left(z_{pi} - \hat{h}_{i,n}\sigma_n - \hat{h}_{i,n+1}\sigma_{n+1}\right)\sigma_{n+1}dt'$$

$$= \frac{1}{6}\Delta t_{n+1}C_{pi}\left[z_{pi} - \hat{h}_{i,n} + 2\left(z_{pi} - \hat{h}_{i,n+1}\right)\right]. \tag{108}$$

2. Head drops below z_{pi} within the time element. This sink function must allow for linear variation of head from $\hat{h}_{i,n}$ to z_{pi} during the time interval t_n to $t_n + \phi_i\Delta t_{n+1}$, after which the sink function vanishes.

$$\int_0^{\Delta t_{n+1}} C_{pi}\left(z_{pi} - \hat{h}_i\right)\sigma_{n+1}dt' = \int_0^{\Delta t_{n+1}} C_{pi}\left(z_{pi} - \hat{h}_{i,n}\sigma_n - \hat{h}_{i,n+1}\sigma_{n+1}\right)\sigma_{n+1}dt'$$

$$= C_{pi}\int_0^{\phi_i\Delta t_{n+1}}\left[z_{pi} - \hat{h}_{i,n}\sigma_n - \left(\left(z_{pi} - \hat{h}_{i,n}\right)\frac{1}{\phi_i} + \hat{h}_{i,n}\right)\sigma_{n+1}\right]\sigma_{n+1}dt'$$

$$= C_{pi}\left(z_{pi} - \hat{h}_{i,n}\right)\int_0^{\phi_i\Delta t_{n+1}}\left(1 - \frac{\sigma_{n+1}}{\phi_i}\right)\sigma_{n+1}dt'$$

$$= \frac{1}{6}\phi_i^2\Delta t_{n+1}C_{pi}\left(z_{pi} - \hat{h}_{i,n}\right), \tag{109}$$

where equation (107) was used to eliminate $\hat{h}_{i,n+1}$.

3. Head rises above z_{pi} within the time element. This sink function must allow for linear variation of head from z_{pi} to $\hat{h}_{i,n+1}$ during the time interval $t_n + \phi_i\Delta_{n+1}$ to t_{n+1}, before which the sink function vanishes.

$$\int_0^{\Delta t_{n+1}} C_{pi}\left(z_{pi} - \hat{h}_i\right)\sigma_{n+1}dt' = \int_0^{\Delta t_{n+1}} C_{pi}\left(z_{pi} - \hat{h}_{i,n}\sigma_n - \hat{h}_{i,n+1}\sigma_{n+1}\right)\sigma_{n+1}dt'$$

$$= C_{pi}\int_{\phi_i\Delta t_{n+1}}^{\Delta t_{n+1}}\left[z_{pi} - \left(z_{pi} - \phi_i\hat{h}_{i,n+1}\right)\frac{\sigma_n}{1 - \phi_i} - \hat{h}_{i,n+1}\sigma_{n+1}\right]\sigma_{n+1}dt'$$

$$= C_{pi}\left(z_{pi} - \hat{h}_{i,n+1}\right)\int_{\phi_i \Delta t_{n+1}}^{\Delta t_{n+1}}\left[1 - \frac{\sigma_n}{1 - \phi_i}\right]\sigma_{n+1}dt'$$

$$= \frac{1}{3}\left(1 - \phi_i'\right)\Delta t_{n+1} C_{pi}\left(z_{pi} - \hat{h}_{i,n+1}\right), \tag{110}$$

where equation (107) was used to eliminate $\hat{h}_{i,n}$, and

$$\phi_i' = \frac{\phi_i\left(\phi_i + 1\right)}{2}, \tag{111}$$

4. Head below z_{pi} throughout the time element. The sink function vanishes during the entire time element.

To obtain the terms that add into equation (71), the results of cases 1 through 4 must be multiplied by $-2/\Delta t_{n+1}$ and converted to residual form using equation (57) to give

1. $-\frac{1}{3}C_{pi}\left[z_{pi} - \hat{h}_{i,n} + 2\left(z_{pi} - \hat{h}_{i,n+1}\right)\right]$

$$= C_{pi}\delta_i - C_{pi}\left(z_{pi} - \hat{h}_{i,n}\right). \tag{112}$$

2. $-\frac{1}{3}\phi_i^2 C_{pi}\left(z_{pi} - \hat{h}_{i,n}\right). \tag{113}$

3. $-\frac{2}{3}\left(1 - \phi_i'\right)C_{pi}\left(z_{pi} - \hat{h}_{i,n+1}\right)$

$$= \left(1 - \phi_i'\right)C_{pi}\delta_i - \frac{2}{3}\left(1 - \phi_i'\right)C_{pi}\left(z_{pi} - \hat{h}_{i,n}\right). \tag{114}$$

4. No formulation.

Addition of these terms into equation (71) consists of adding the coefficient of δ_i (that is, C_{pi} or $(1 - \phi_i')C_{pi}$) into matrix $\underline{\underline{V}}$ and adding the term containing $z_{pi} - \hat{h}_{i,n}$ onto the right-hand side. Because ϕ_i is unknown at the beginning of the time element, the predictor-corrector method is used to solve the modified equation (71).

The predictor step is initiated by checking whether $\hat{h}_{i,n} \geq z_{pi}$ or $\hat{h}_{i,n} < z_{pi}$. If the former is true, then case 1 is assumed and if the latter is true, then case 4 is assumed. Prediction equation (76) is then solved with the appropriate terms added in, and predicted heads $\underline{\hat{h}}^*$ are obtained using equation (79).

39

H = hydraulic head at top of confining unit or riverbed

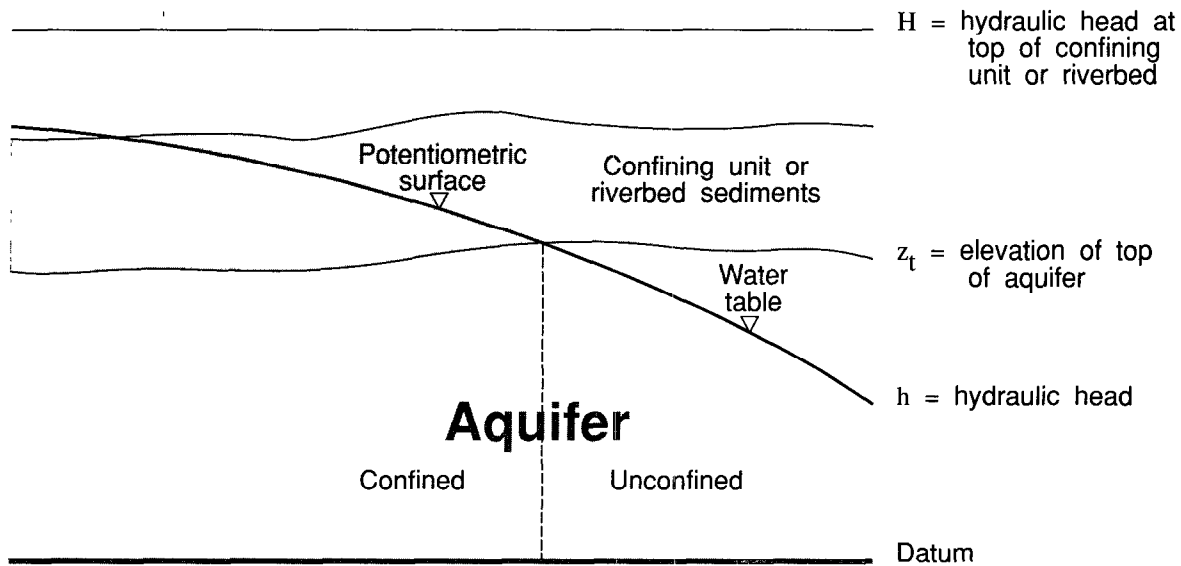z_t = elevation of top of aquifer

h = hydraulic head

Figure 11. Cross section showing aquifer dewatering beneath a confining unit or riverbed sediments having low permeability.

To initiate the corrector step, heads $\hat{h}_i^*$ and $\hat{h}_{i,n}$ are checked to determine which of cases 1 through 4 apply. If case 2 or case 3 applies, then ϕ_i is estimated from

$$\phi_i = \frac{z_{pi} - \hat{h}_{i,n}}{\hat{h}_i^* - \hat{h}_{i,n}}. \tag{115}$$

Predicted head $\hat{h}_i^*$ was found to be a good prediction of $\hat{h}_{i,n+1}$ unless the time-element size was too large. The corrector equation is formed by adding the appropriate terms into equation (80), in which $\tilde{G}^*$ and $\underline{G}^*$ may or may not be time variant depending on whether flow is unconfined or confined.

Areal head-dependent leakage combined with aquifer dewatering

Vertical leakage through a confining unit overlying an aquifer being dewatered, or leakage through the bed materials (assumed to have low permeability) of a river that is wide enough that it cannot be considered to be a line source or sink, may be simulated using a function in equation (1) similar to R(H - h) (figure 11) (Prickett and Lonnquist, 1971, p. 33-35). The difference is that in the present case the maximum rate of leakage to the aquifer is attained when the head in the aquifer declines below the base of the overlying confining unit or riverbed sediments. Any further decline in head results in a constant rate of leakage. There is no maximum rate of leakage from the aquifer when the head rises above the base of the confining unit or riverbed sediments. With this leakage function included, equation (1) may be written as

$$\frac{\partial}{\partial x}\left(T_{xx}\frac{\partial h}{\partial x} + T_{xy}\frac{\partial h}{\partial y}\right) + \frac{\partial}{\partial y}\left(T_{yx}\frac{\partial h}{\partial x} + T_{yy}\frac{\partial h}{\partial y}\right)$$
$$+ R(H - h) + S_a + W + P = S\frac{\partial h}{\partial t}, \tag{116}$$

40

where

$$S_a = \begin{cases} R_a \left(H_a - h \right), & h > z_t \\ R_a \left(H_a - z_t \right), & h \leq z_t \end{cases} \qquad (117)$$

In equation (117), R_a is the hydraulic conductance [time^{-1}] of the confining unit or riverbed sediments overlying the aquifer, H_a is the head at the distal side of the confining unit or riverbed sediments, and z_t is the elevation of the base of the overlying confining unit or riverbed sediments. The term $R(H - h)$ is retained in equation (116) to allow for a confining unit underlying the aquifer.

Spatial finite-element discretization applied to equation (117) results in an equation analogous to equation (27). Therefore, the leakage term resulting from the patch of elements for node i can be written

$$Q_{ai} = \begin{cases} C_{ai} \left(H_{ai} - \hat{h}_i \right), & \hat{h}_i > z_{ti} \\ C_{ai} \left(H_{ai} - z_{ti} \right), & \hat{h}_i \leq z_{ti} \end{cases} \qquad (118)$$

where

$$C_{ai} = \frac{1}{3} \sum_{e_i} R_a^e \Delta^e, \qquad (119)$$

and Q_{ai} is the volumetric flow rate at node i [length^3/time] from leakage through the overlying confining unit or riverbed sediments.

Four cases similar to those developed for the point head-dependent sink functions (figure 10) are used to integrate equation (118) over time. The time element is divided in the same manner into two subintervals if the head in the aquifer crosses the base of the overlying confining unit or riverbed sediments within the element. For convenience, the same designation ϕ_i is used for the changeover point in time. The four cases can be expressed as follows:

1. Head above z_{ti} throughout the time element.

$$\int_0^{\Delta t_{n+1}} C_{ai} \left(H_{ai} - \hat{h}_i \right) \sigma_{n+1} dt'$$

$$= C_{ai} \int_0^{\Delta t_{n+1}} \left[\left(H_{ai,n} - \hat{h}_{i,n} \right) \sigma_n + \left(H_{ai,n+1} - \hat{h}_{i,n+1} \right) \sigma_{n+1} \right] \sigma_{n+1} dt'$$

$$= \frac{1}{6} \Delta t_{n+1} C_{ai} \left[H_{ai,n} - \hat{h}_{i,n} + 2 \left(H_{ai,n+1} - \hat{h}_{i,n+1} \right) \right] \qquad (120)$$

41

2. Head drops below z_{ti} within the time element. This function must allow for linear variation of head from $\hat{h}_{i,n}$ to z_{ti} during time interval t_n to $t_n + \phi_i \Delta t_{n+1}$, after which the head-dependent function is replaced by a known function.

$$\int_0^{\phi_i \Delta t_{n+1}} C_{ai}\left(H_{ai} - \hat{h}_i\right)\sigma_{n+1}dt' + \int_{\phi_i \Delta t_{n+1}}^{\Delta t_{n+1}} C_{ai}\left(H_{ai} - z_{ti}\right)\sigma_{n+1}dt'$$

$$= \int_0^{\Delta t_{n+1}} C_{ai}H_{ai}\sigma_{n+1}dt' - \int_0^{\phi_i \Delta t_{n+1}} C_{ai}\hat{h}_i\sigma_{n+1}dt' - \int_{\phi_i \Delta t_{n+1}}^{\Delta t_{n+1}} C_{ai}z_{ti}\sigma_{n+1}dt'$$

$$= C_{ai}\int_0^{\Delta t_{n+1}} \left(H_{ai,n}\sigma_n + H_{ai,n+1}\sigma_{n+1}\right)\sigma_{n+1}dt'$$

$$- C_{ai}\int_0^{\phi_i \Delta t_{n+1}} \left[\hat{h}_{i,n}\sigma_n + \left(\left(z_{ti} - \hat{h}_{i,n}\right)\frac{1}{\phi_i} + \hat{h}_{i,n}\right)\sigma_{n+1}\right]\sigma_{n+1}dt'$$

$$- C_{ai}z_{ti}\int_{\phi_i \Delta t_{n+1}}^{\Delta t_{n+1}} \sigma_{n+1}dt'$$

$$= \frac{1}{6}\phi_i^2 \Delta t_{n+1}C_{ai}\left[H_{ai,n} - \hat{h}_{i,n} + 2\left(H_{ai,n+1} - z_{ti}\right)\right]$$

$$+ \frac{1}{6}\left(1 - \phi_i^2\right)\Delta t_{n+1}C_{ai}\left[H_{ai,n} - z_{ti} + 2\left(H_{ai,n+1} - z_{ti}\right)\right], \qquad (121)$$

where equation (107) was used to eliminate $\hat{h}_{i,n+1}$.

3. Head rises above z_{ti} within the time element. This function must allow for linear variation of head from z_{ti} to $\hat{h}_{i,n+1}$ during the time interval $t_n + \phi_i \Delta t_{n+1}$ to t_{n+1}, before which the head dependent function is replaced by a known function.

$$\int_0^{\phi_i \Delta t_{n+1}} C_{ai}\left(H_{ai} - z_{ti}\right)\sigma_{n+1} dt' + \int_{\phi_i \Delta t_{n+1}}^{\Delta t_{n+1}} C_{ai}\left(H_{ai} - \hat{h}_i\right)\sigma_{n+1} dt'$$

$$= \int_0^{\Delta t_{n+1}} C_{ai}H_{ai}\sigma_{n+1} dt' - \int_0^{\phi_i \Delta t_{n+1}} C_{ai}z_{ti}\sigma_{n+1} dt' - \int_{\phi_i \Delta t_{n+1}}^{\Delta t_{n+1}} C_{ai}\hat{h}_i\sigma_{n+1} dt'$$

$$= C_{ai}\int_0^{\Delta t_{n+1}} \left(H_{ai,n}\sigma_n + H_{ai,n+1}\sigma_{n+1}\right)\sigma_{n+1} dt' - C_{ai}z_{ti}\int_0^{\phi_i \Delta t_{n+1}} \sigma_{n+1} dt'$$

$$- C_{ai}\int_{\phi_i \Delta t_{n+1}}^{\Delta t_{n+1}} \left[\left(z_{ti} - \phi_i\hat{h}_{i,n+1}\right)\frac{\sigma_n}{1-\phi_i} + \hat{h}_{i,n+1}\sigma_{n+1}\right]\sigma_{n+1} dt'$$

$$= \frac{1}{6}\phi_i' \Delta t_{n+1}C_{ai}\left[H_{ai,n} - z_{ti} + 2\left(H_{ai,n+1} - z_{ti}\right)\right]$$

$$+ \frac{1}{6}\left(1 - \phi_i'\right)\Delta t_{n+1}C_{ai}\left[H_{ai,n} - z_{ti} + 2\left(H_{ai,n+1} - \hat{h}_{i,n+1}\right)\right], \qquad (122)$$

where equation (107) was used to eliminate $\hat{h}_{i,n}$, and ϕ_i' is defined by equation (111).

4. Head below z_{ti} throughout the time element.

$$\int_0^{\Delta t_{n+1}} C_{ai}\left(H_{ai} - z_{ti}\right)\sigma_{n+1} dt'$$

$$= C_{ai}\int_0^{\Delta t_{n+1}} \left[\left(H_{ai,n} - z_{ti}\right)\sigma_n + \left(H_{ai,n+1} - z_{ti}\right)\sigma_{n+1}\right]\sigma_{n+1} dt'$$

$$= \frac{1}{6}\Delta t_{n+1}C_{ai}\left[H_{ai,n} - z_{ti} + 2\left(H_{ai,n+1} - z_{ti}\right)\right]. \qquad (123)$$

As for the point head-dependent sink functions, the terms that add into equation (71) are obtained by multiplying the above results by $-2/\Delta t_{n+1}$ and converting to residual form using equation (57). The results are:

1. $-\frac{1}{3}C_{ai}\left[H_{ai,n} - \hat{h}_{i,n} + 2\left(H_{ai,n+1} - \hat{h}_{i,n+1}\right)\right]$

$$= C_{ai}\delta_i - \frac{1}{3}C_{ai}\left[H_{ai,n} - \hat{h}_{i,n} + 2\left(H_{ai,n+1} - \hat{h}_{i,n}\right)\right]. \qquad (124)$$

2. $-\frac{1}{3}\phi_i^2 C_{ai}\left[H_{ai,n} - \hat{h}_{i,n} + 2\left(H_{ai,n+1} - z_{ti}\right)\right]$

$$-\frac{1}{3}\left(1 - \phi_i^2\right)C_{ai}\left[H_{ai,n} - z_{ti} + 2\left(H_{ai,n+1} - z_{ti}\right)\right]. \qquad (125)$$

3. $-\frac{1}{3}\phi_i' C_{ai}\left[H_{ai,n} - z_{ti} + 2\left(H_{ai,n+1} - z_{ti}\right)\right]$

$$-\frac{1}{3}\left(1 - \phi_i'\right)C_{ai}\left[H_{ai,n} - z_{ti} + 2\left(H_{ai,n+1} - \hat{h}_{i,n+1}\right)\right]$$

$$= \left(1 - \phi_i'\right)C_{ai}\delta_i - \frac{1}{3}\phi_i' C_{ai}\left[H_{ai,n} - z_{ti} + 2\left(H_{ai,n+1} - z_{ti}\right)\right]$$

$$-\frac{1}{3}\left(1 - \phi_i'\right)C_{ai}\left[H_{ai,n} - z_{ti} + 2\left(H_{ai,n+1} - \hat{h}_{i,n}\right)\right]. \qquad (126)$$

4. $$-\frac{1}{3}C_{ai}\left[H_{ai,n} - z_{ti} + 2\left(H_{ai,n+1} - z_{ti}\right)\right]. \qquad (127)$$

The terms in the above four cases are incorporated into equation (71) and the predictor-corrector method is employed in exactly the same manner as for the point head-dependent sink functions.

Areal head-dependent discharge (evapotranspiration)

Another areally distributed function allows for discharge-only processes such as evapotranspiration (figure 12). The rate of discharge from the aquifer is assumed to reach a maximum when the water table (or head in the aquifer) reaches the top of the aquifer, which is land surface. The minimum rate of zero is reached when the head declines to some lower threshold elevation (Prickett and Lonnquist, 1971, p. 37-38). This discharge function occupies the same position in equation (1) as S_a (see equation (116)) and is stated in the form

$$S_e = \begin{cases} R_e\left(z_e - z_t\right), & h \geq z_t \\ R_e\left(z_e - h\right), & z_e < h < z_t, \\ 0 & , h \leq z_e \end{cases} \qquad (128)$$

where R_e linearly relates the discharge rate to the head difference, z_e is the elevation below which the function vanishes, z_t is the elevation of the top of the aquifer, and $z_t > z_e$. An expression for R_e is (Prickett and Lonnquist, 1971, p. 37)

44

$$R_e = \frac{v_e}{d_e},$$ (129)

where

$$d_e = z_t - z_e,$$ (130)

and v_e is the absolute value of the maximum unit discharge rate [length/time] due to evapotranspiration from the aquifer.

Spatial integration of equation (128) is performed by using the same process used for equations (118) and (119). Therefore,

$$Q_{ei} = \begin{cases} C_{ei}\left(z_{ei} - z_{ti}\right), & \hat{h}_i \geq z_{ti} \\ C_{ei}\left(z_{ei} - \hat{h}_i\right), & z_{ei} < \hat{h}_i < z_{ti}, \\ 0 & , \hat{h}_i \leq z_{ei} \end{cases}$$ (131)

where

$$C_{ei} = \frac{1}{3}\sum_{i} R_e^e \Delta^e,$$ (132)

and Q_{ei} is volumetric discharge at node i [length^3/time].

Time integration yields nine separate cases (figure 13) involving the positions of $\hat{h}_{i,n}$ and $\hat{h}_{i,n+1}$ relative to z_{ei} and z_{ti}, and the time element is divided into either one, two, or three subintervals depending on the case applying. Changeover points in time are designated ϕ_{ti} and ϕ_{ei} to conform with the changeover elevations z_{ti} and z_{ei}, so that
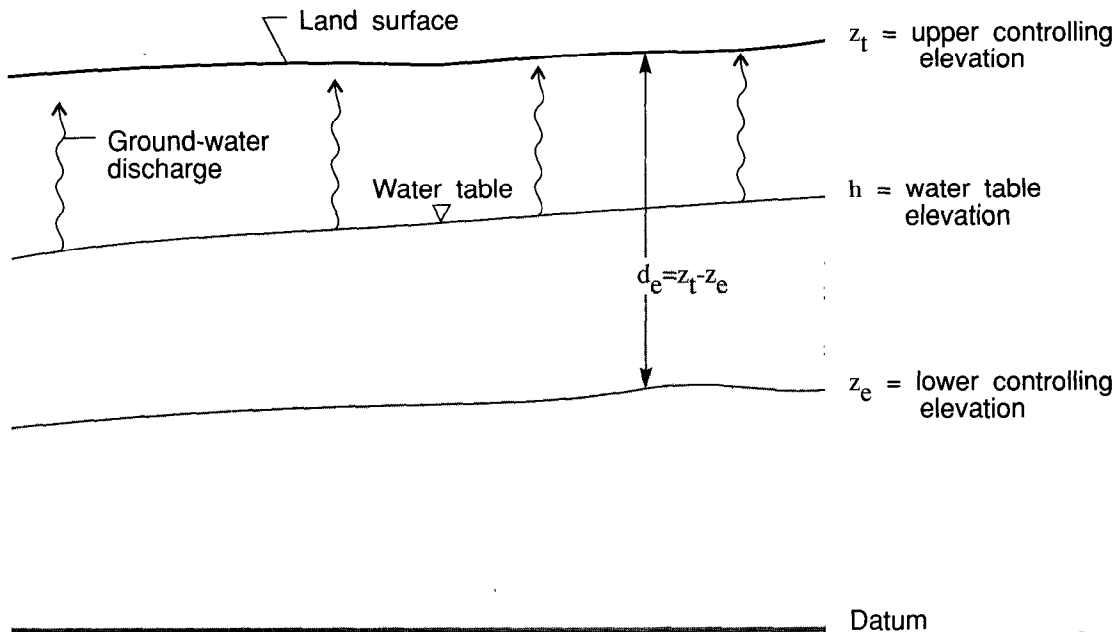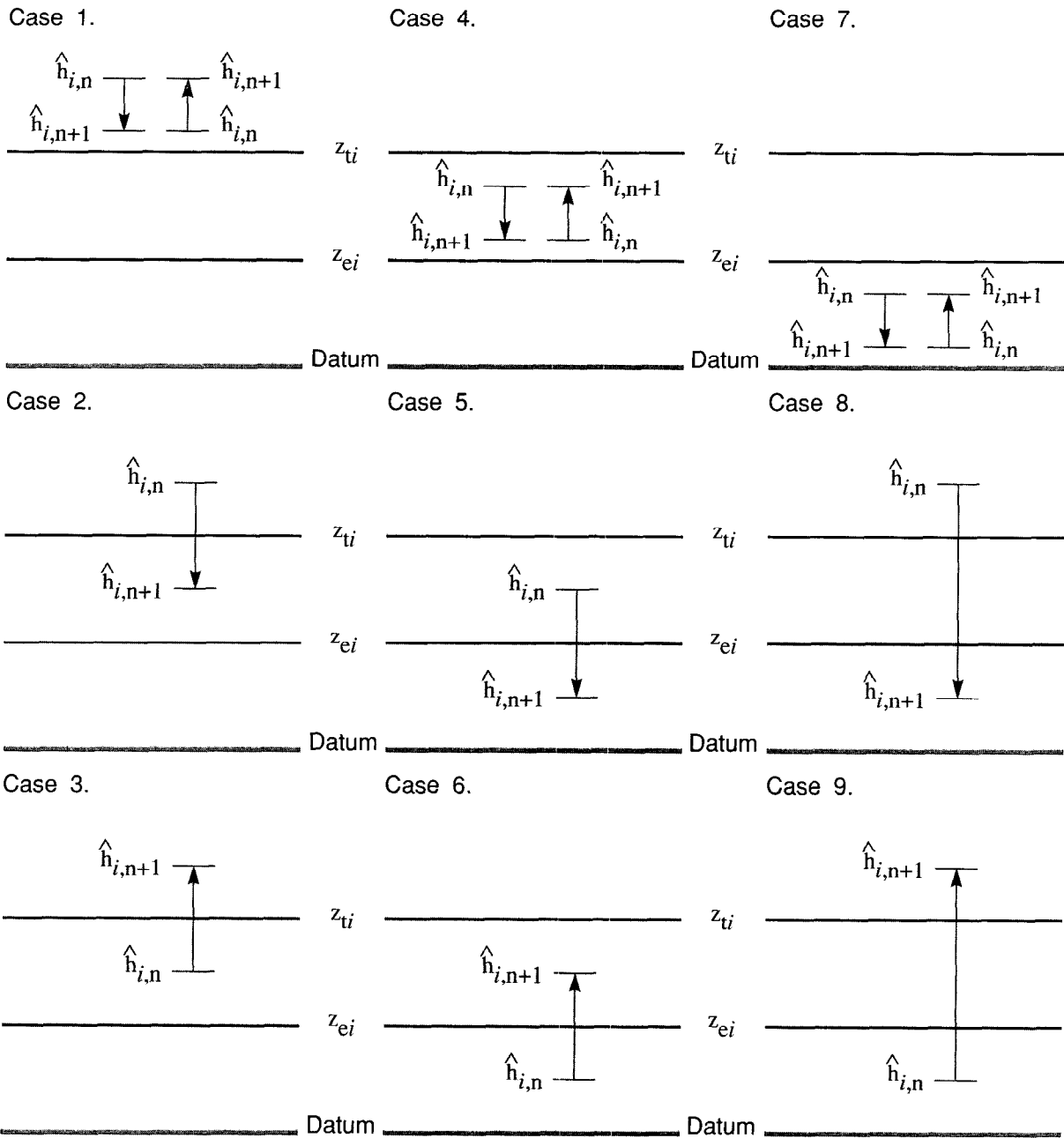

Figure 12. Cross section showing configuration of the water table and controlling elevations for evapotranspiration type of head-dependent discharge.

45

Case 1.   Case 4.   Case 7.

$\hat{h}_{i,n}$ ——— ——— $\hat{h}_{i,n+1}$

$\hat{h}_{i,n+1}$ ——— ——— $\hat{h}_{i,n}$

——————————— z_{ti} ——————————— z_{ti} ———————————

                         $\hat{h}_{i,n}$ ——— ——— $\hat{h}_{i,n+1}$

                         $\hat{h}_{i,n+1}$ ——— ——— $\hat{h}_{i,n}$

——————————— z_{ei} ——————————— z_{ei} ———————————

                                                   $\hat{h}_{i,n}$ ——— ——— $\hat{h}_{i,n+1}$

                                                   $\hat{h}_{i,n+1}$ ——— ——— $\hat{h}_{i,n}$

═════════════ Datum   ═════════════ Datum   ═════════════

Case 2.   Case 5.   Case 8.

$\hat{h}_{i,n}$ ——— $\hat{h}_{i,n}$ ———

——————————— z_{ti} ——————————— z_{ti} ———————————

                         $\hat{h}_{i,n}$ ———

$\hat{h}_{i,n+1}$ ———

——————————— z_{ei} ——————————— z_{ei} ———————————

                         $\hat{h}_{i,n+1}$ ———

                                                   $\hat{h}_{i,n+1}$ ———

═════════════ Datum   ═════════════ Datum   ═════════════

Case 3.   Case 6.   Case 9.

$\hat{h}_{i,n+1}$ ——— $\hat{h}_{i,n+1}$ ———

——————————— z_{ti} ——————————— z_{ti} ———————————

$\hat{h}_{i,n}$ ——— $\hat{h}_{i,n+1}$ ———

——————————— z_{ei} ——————————— z_{ei} ———————————

                         $\hat{h}_{i,n}$ ——— $\hat{h}_{i,n}$ ———

═════════════ Datum   ═════════════ Datum   ═════════════

z_{ti} = upper controlling elevation at node i

z_{ei} = lower controlling elevation at node i

$\hat{h}_{i,r}$ (r=n,n+1) = hydraulic head at node i and at time level r

Figure 13. Nine possible cases involving change in head over time-element n+1 during which there is areal head-dependent discharge.

46

$$\phi_{ti} = \frac{z_{ti} - \hat{h}_{i,n}}{\hat{h}_{i,n+1} - \hat{h}_{i,n}}, \tag{133}$$

and

$$\phi_{ei} = \frac{z_{ei} - \hat{h}_{i,n}}{\hat{h}_{i,n+1} - \hat{h}_{i,n}}. \tag{134}$$

The cases are as follows.

1. Head above z_{ti} throughout the time element.

$$\int_0^{\Delta t_{n+1}} C_{ei}\left(z_{ei} - z_{ti}\right)\sigma_{n+1} dt' = \frac{1}{2}\Delta t_{n+1} C_{ei}\left(z_{ei} - z_{ti}\right). \tag{135}$$

2. Head drops below z_{ti} but stays above z_{ei} within the time element.

$$\int_0^{\phi_{ti}\Delta t_{n+1}} C_{ei}\left(z_{ei} - z_{ti}\right)\sigma_{n+1} dt' + \int_{\phi_{ti}\Delta t_{n+1}}^{\Delta t_{n+1}} C_{ei}\left(z_{ei} - \hat{h}_i\right)\sigma_{n+1} dt'$$

$$= C_{ei}\left(z_{ei} - z_{ti}\right)\int_0^{\phi_{ti}\Delta t_{n+1}} \sigma_{n+1} dt'$$

$$+ C_{ei}\int_{\phi_{ti}\Delta t_{n+1}}^{\Delta t_{n+1}} \left[z_{ei} - \left(z_{ti} - \phi_{ti}\hat{h}_{i,n+1}\right)\frac{\sigma_n}{1 - \phi_{ti}} - \hat{h}_{i,n+1}\sigma_{n+1}\right]\sigma_{n+1} dt'$$

$$= \frac{1}{2}\phi'_{ti}\Delta t_{n+1}C_{ei}\left(z_{ei} - z_{ti}\right) + \frac{1}{6}\left(1 - \phi'_{ti}\right)\Delta t_{n+1}C_{ei}\left[z_{ei} - z_{ti} + 2\left(z_{ei} - \hat{h}_{i,n+1}\right)\right], \tag{136}$$

where ϕ'_{ti} is given by equation (111) with ϕ_{ti} replacing ϕ_i.

3. Head rises from between z_{ei} and z_{ti} to above z_{ti} within the time element.

$$\int_0^{\phi_{ti}\Delta t_{n+1}} C_{ei}\left(z_{ei} - \hat{h}_i\right)\sigma_{n+1} dt' + \int_{\phi_{ti}\Delta t_{n+1}}^{\Delta t_{n+1}} C_{ei}\left(z_{ei} - z_{ti}\right)\sigma_{n+1} dt'$$

$$= C_{ei} \int_0^{\phi_{ti}\Delta t_{n+1}} \left[z_{ei} - \hat{h}_{i,n}\sigma_n - \left(\left(z_{ti} - \hat{h}_{i,n} \right)\frac{1}{\phi_{ti}} + \hat{h}_{i,n} \right)\sigma_{n+1} \right]\sigma_{n+1}dt'$$

$$+ C_{ei}\left(z_{ei} - z_{ti} \right) \int_{\phi_{ti}\Delta t_{n+1}}^{\Delta t_{n+1}} \sigma_{n+1}dt'$$

$$= \frac{1}{6}\phi_{ti}^2\Delta t_{n+1}C_{ei}\left[z_{ei} - \hat{h}_{i,n} + 2\left(z_{ei} - z_{ti} \right) \right] + \frac{1}{2}\left(1 - \phi_{ti}^2 \right)\Delta t_{n+1}C_{ei}\left(z_{ei} - z_{ti} \right). \quad (137)$$

4. Head stays between z_{ei} and z_{ti} throughout the time element.

$$\int_0^{\Delta t_{n+1}} C_{ei}\left(z_{ei} - \hat{h}_i \right)\sigma_{n+1}dt' = C_{ei} \int_0^{\Delta t_{n+1}} \left[\left(z_{ei} - \hat{h}_{i,n} \right)\sigma_n + \left(z_{ei} - \hat{h}_{i,n+1} \right)\sigma_{n+1} \right]\sigma_{n+1}dt'$$

$$= \frac{1}{6}\Delta t_{n+1}C_{ei}\left[z_{ei} - \hat{h}_{i,n} + 2\left(z_{ei} - \hat{h}_{i,n+1} \right) \right]. \quad (138)$$

5. Head drops from between z_{ei} and z_{ti} to below z_{ei} within the time element.

$$\int_0^{\phi_{ei}\Delta t_{n+1}} C_{ei}\left(z_{ei} - \hat{h}_i \right)\sigma_{n+1}dt'$$

$$= C_{ei} \int_0^{\phi_{ei}\Delta t_{n+1}} \left[z_{ei} - \hat{h}_{i,n}\sigma_n - \left(\left(z_{ei} - \hat{h}_{i,n} \right)\frac{1}{\phi_{ei}} + \hat{h}_{i,n} \right)\sigma_{n+1} \right]\sigma_{n+1}dt'$$

$$= \frac{1}{6}\phi_{ei}^2\Delta t_{n+1}C_{ei}\left(z_{ei} - \hat{h}_{i,n} \right). \quad (139)$$

48

6. Head rises above z_{ei} but stays below z_t within the time element.

$$\int_{\phi_{ei}\Delta t_{n+1}}^{\Delta t_{n+1}} C_{ei}\left(z_{ei} - \hat{h}_i\right)\sigma_{n+1}dt' = C_{ei}\int_{\phi_{ei}\Delta t_{n+1}}^{\Delta t_{n+1}} \left[z_{ei} - \left(z_{ei} - \phi_{ei}\hat{h}_{i,n+1}\right)\frac{\sigma_n}{1-\phi_{ei}}\right.$$

$$\left. - \hat{h}_{i,n+1}\sigma_{n+1}\right]\sigma_{n+1}dt' = \frac{1}{3}\left(1 - \phi'_{ei}\right)\Delta t_{n+1}C_{ei}\left(z_{ei} - \hat{h}_{i,n+1}\right), \qquad (140)$$

where ϕ'_{ei} is given by equation (111) with ϕ_{ei} replacing ϕ_i.

7. Head stays below z_{ei} throughout the time element. The discharge function vanishes within the entire time element.

8. Head drops from above z_{ti} to below z_{ei} within the time element. This function must allow for constant discharge during timespan t_n to $t_n + \phi_{ti}\Delta t_{n+1}$ and head-dependent discharge during timespan $t_n + \phi_{ti}\Delta t_{n+1}$ to $t_n + \phi_{ei}\Delta t_{n+1}$, and must vanish during timespan $t_n + \phi_{ei}\Delta t_{n+1}$ to t_{n+1}. The head-dependent discharge can be expressed as a function of ϕ_{ei}, ϕ_{ti}, z_{ei}, and z_{ti} by eliminating $\hat{h}_{i,n}$ and $\hat{h}_{i,n+1}$ using equations (133) and (134). First $\hat{h}_{i,n+1}$ is eliminated by solving equation (134) for $\hat{h}_{i,n+1}$, then $\hat{h}_{i,n}$ is eliminated by combining equations (133) and (134) to get

$$\hat{h}_{i,n} = \frac{\phi_{ei}z_{ti} - \phi_{ti}z_{ei}}{\phi_{ei} - \phi_{ti}} \qquad (141)$$

Thus,

$$\int_0^{\phi_{ti}\Delta t_{n+1}} C_{ei}\left(z_{ei} - z_{ti}\right)\sigma_{n+1}dt' + \int_{\phi_{ti}\Delta t_{n+1}}^{\phi_{ei}\Delta t_{n+1}} C_{ei}\left(z_{ei} - \hat{h}_i\right)\sigma_{n+1}dt'$$

$$= C_{ei}\left(z_{ei} - z_{ti}\right)\int_0^{\phi_{ti}\Delta t_{n+1}} \sigma_{n+1}dt' + C_{ei}\int_{\phi_{ti}\Delta t_{n+1}}^{\phi_{ei}\Delta t_{n+1}} \left[z_{ei} - \hat{h}_{i,n}\sigma_n - \left(\left(z_{ei} - \hat{h}_{i,n}\right)\cdot\right.\right.$$

$$\left.\left. \cdot \frac{1}{\phi_{ei}} + \hat{h}_{i,n}\right)\sigma_{n+1}\right]\sigma_{n+1}dt'$$

$$= C_{ei}\left(z_{ei} - z_{ti}\right) \int_0^{\phi_{ti}\Delta t_{n+1}} \sigma_{n+1} dt' + C_{ei}\left(z_{ei} - \hat{h}_{i,n}\right) \int_{\phi_{ti}\Delta t_{n+1}}^{\phi_{ei}\Delta t_{n+1}} \left(1 - \frac{\sigma_{n+1}}{\phi_{ei}}\right)\sigma_{n+1} dt'$$

$$= C_{ei}\left(z_{ei} - z_{ti}\right) \int_0^{\phi_{ti}\Delta t_{n+1}} \sigma_{n+1} dt' + C_{ei}\left(z_{ei} - z_{ti}\right) \int_{\phi_{ti}\Delta t_{n+1}}^{\phi_{ei}\Delta t_{n+1}} \left(\frac{\phi_{ei} - \sigma_{n+1}}{\phi_{ei} - \phi_{ti}}\right)\sigma_{n+1} dt'$$

$$= \frac{1}{6}\left[\phi_{ti}\left(\phi_{ei} + \phi_{ti}\right) + \phi_{ei}^2\right]\Delta t_{n+1} C_{ei}\left(z_{ei} - z_{ti}\right). \qquad (142)$$

9. Head rises from below z_{ei} to above z_{ti} within the time element. This case is analogous to case 8, except that the head changes in the opposite direction. Hence, the resulting equations are

$$\int_{\phi_{ei}\Delta t_{n+1}}^{\phi_{ti}\Delta t_{n+1}} C_{ei}\left(z_{ei} - \hat{h}_i\right)\sigma_{n+1} dt' + \int_{\phi_{ti}\Delta t_{n+1}}^{\Delta t_{n+1}} C_{ei}\left(z_{ei} - z_{ti}\right)\sigma_{n+1} dt'$$

$$= C_{ei}\left(z_{ei} - z_{ti}\right) \int_{\phi_{ei}\Delta t_{n+1}}^{\phi_{ti}\Delta t_{n+1}} \left(\frac{\phi_{ei} - \sigma_{n+1}}{\phi_{ei} - \phi_{ti}}\right)\sigma_{n+1} dt' + C_{ei}\left(z_{ei} - z_{ti}\right) \int_{\phi_{ti}\Delta t_{n+1}}^{\Delta t_{n+1}} \sigma_{n+1} dt'$$

$$= \frac{1}{6}\left[\left(\phi_{ei} + 2\phi_{ti}\right)\left(\phi_{ti} - \phi_{ei}\right) + 3\left(1 + \phi_{ti}\right)\left(1 - \phi_{ti}\right)\right]\Delta t_{n+1} C_{ei}\left(z_{ei} - z_{ti}\right). \qquad (143)$$

Multiplication of the above discharge functions by $-2/\Delta t_{n+1}$ and conversion to residual form using equation (57) yields the terms that add into equation (71). The results are:

1. $\quad -C_{ei}\left(z_{ei} - z_{ti}\right).$ \hfill (144)

2. $\quad -\phi'_{ti}C_{ei}\left(z_{ei} - z_{ti}\right) - \frac{1}{3}\left(1 - \phi'_{ti}\right)C_{ei}\left[z_{ei} - z_{ti} + 2\left(z_{ei} - \hat{h}_{i,n+1}\right)\right]$

$$= \left(1 - \phi'_{ti}\right)C_{ei}\delta_i - \phi'_{ti}C_{ei}\left(z_{ei} - z_{ti}\right) - \frac{1}{3}\left(1 - \phi'_{ti}\right)C_{ei}\left[z_{ei} - z_{ti}\right.$$

$$\left. + 2\left(z_{ei} - \hat{h}_{i,n}\right)\right]. \qquad (145)$$

50

3. $\quad -\frac{1}{3}\phi_{ti}^2 C_{ei}\left[z_{ei} - \hat{h}_{i,n} + 2\left(z_{ei} - z_{ti}\right)\right] - \left(1 - \phi_{ti}^2\right)C_{ei}\left(z_{ei} - z_{ti}\right).$ (146)

4. $\quad -\frac{1}{3}C_{ei}\left[z_{ei} - \hat{h}_{i,n} + 2\left(z_{ei} - \hat{h}_{i,n+1}\right)\right]$

$\quad = C_{ei}\delta_i - C_{ei}\left(z_{ei} - \hat{h}_{i,n}\right).$ (147)

5. $\quad -\frac{1}{3}\phi_{ei}^2 C_{ei}\left(z_{ei} - \hat{h}_{i,n}\right).$ (148)

6. $\quad -\frac{2}{3}\left(1 - \phi_{ei}'\right)C_{ei}\left(z_{ei} - \hat{h}_{i,n+1}\right)$

$\quad = \left(1 - \phi_{ei}'\right)C_{ei}\delta_i - \frac{2}{3}\left(1 - \phi_{ei}'\right)C_{ei}\left(z_{ei} - \hat{h}_{i,n}\right).$ (149)

7. No formulation.

8. $\quad -\frac{1}{3}\left[\phi_{ti}\left(\phi_{ei} + \phi_{ti}\right) + \phi_{ei}^2\right]C_{ei}\left(z_{ei} - z_{ti}\right).$ (150)

9. $\quad -\frac{1}{3}\left[\left(\phi_{ei} + 2\phi_{ti}\right)\left(\phi_{ti} - \phi_{ei}\right) + 3\left(1 + \phi_{ti}\right)\left(1 - \phi_{ti}\right)\right]C_{ei}\left(z_{ei} - z_{ti}\right).$ (151)

Procedures for use of the above nine cases in equation (71) and solution using the predictor-corrector method are analogous to those used for the previous two types of head-dependent functions. For the predictor, if $\hat{h}_{i,n} \geq z_{ti}$, then equation (144) is used in equation (76) (case 1); if $z_{ei} < \hat{h}_{i,n} < z_{ti}$, then equation (147) is used (case 4); and if $\hat{h}_{i,n} \leq z_{ti}$, then no terms are used (case 7). Estimates of ϕ_{ei} and ϕ_{ti} to use in equations (144) through (151) are obtained using equations (133) and (134), with $\hat{h}_i^*$ substituted for $\hat{h}_{i,n+1}$. The corrector is employed by adding one of equations (144) through (151) into corrector equation (80), as appropriate based on checking $\hat{h}_i^*$ and $\hat{h}_{i,n}$ against z_{ei} and z_{ti}, and solving for $\underline{\delta}$.

Line head-dependent leakage combined with aquifer dewatering

The final type of head-dependent function is a line source or sink of the general form of the boundary condition given by equation (4), except in the present case the function yields a maximum flux when the head in the
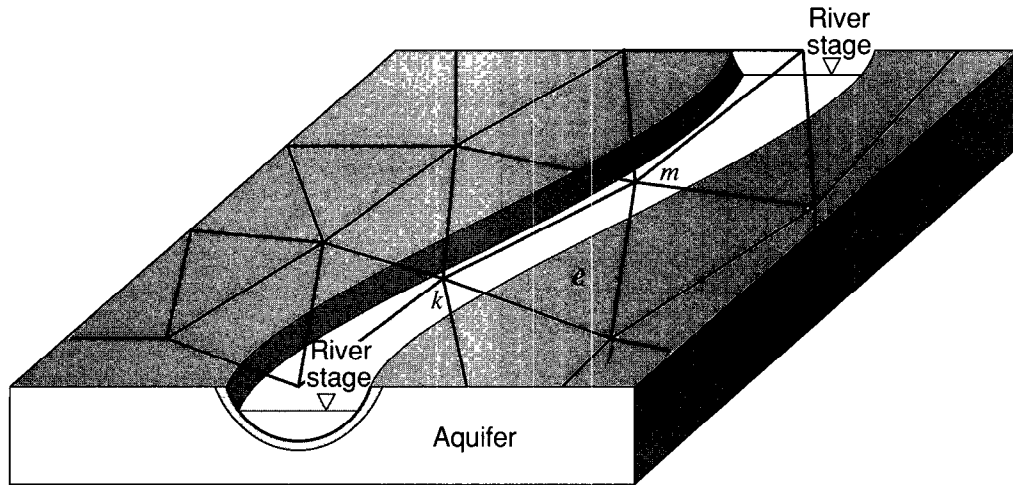
51

Figure 14a. Block diagram of a river idealized as a line source or sink along spatial element sides.

aquifer declines to a specified elevation. This function is most often used to simulate a river that is narrow enough to be replaced by a line (figure 14a). As for the case of a wide river, the maximum leakage rate from the river to the aquifer is attained when the head in the aquifer declines to the bottom of the riverbed sediments (assumed to have low permeability) (figure 14b).

The line source or sink function is written in the form of a flow across an internal or external boundary, or

$$q_n = \begin{cases} \alpha_r \left(H_r - h \right) , & h > z_r \\ \alpha_r \left(H_r - z_r \right), & h \leq z_r \end{cases} , \qquad (152)$$

where α_r [length/time] is a parameter that is a function of the hydraulic conductivity of sediments through which leakage occurs, H_r is the controlling head (for rivers, the river-stage elevation), and z_r is the elevation at which the discharge to the aquifer is a maximum (for rivers, the elevation of the bottom of the riverbed sediments). For riverbed sediments, α_r is given by

$$\alpha_r = \frac{K_r W_r}{b_r} , \qquad (153)$$

where K_r is the hydraulic conductivity of the riverbed sediments, W_r is the width of the river, and b_r is the thickness of the riverbed sediments.

Equation (152) is incorporated into the spatial finite-element equations in the same manner as equation (4) (see equation (32)). That is, the total discharge across the line source or sink in the patch of elements for node i is

$$Q_{ri} = \begin{cases} C_{ri} \left(H_{ri} - \hat{h}_i \right) , & \hat{h}_i > z_{ri} \\ C_{ri} \left(H_{ri} - z_{ri} \right), & \hat{h}_i \leq z_{ri} \end{cases} , \qquad (154)$$
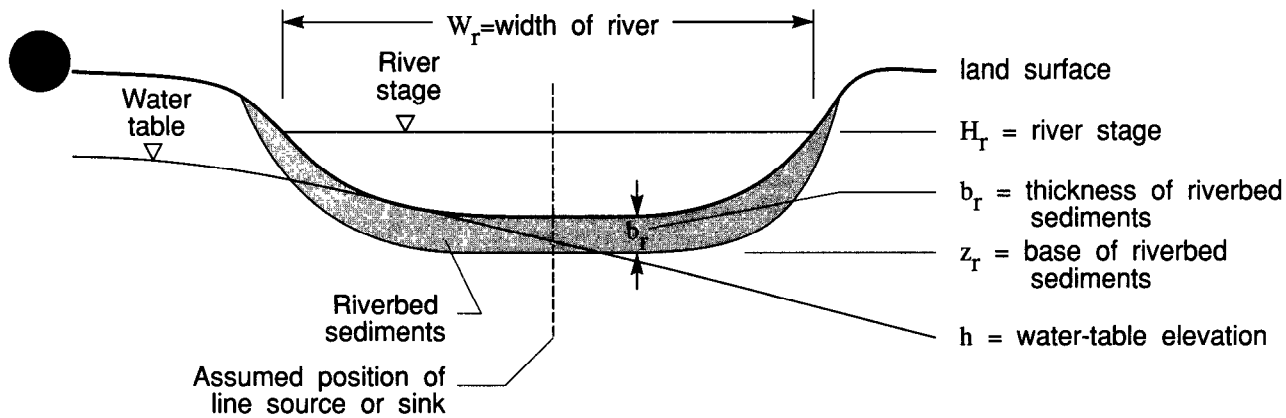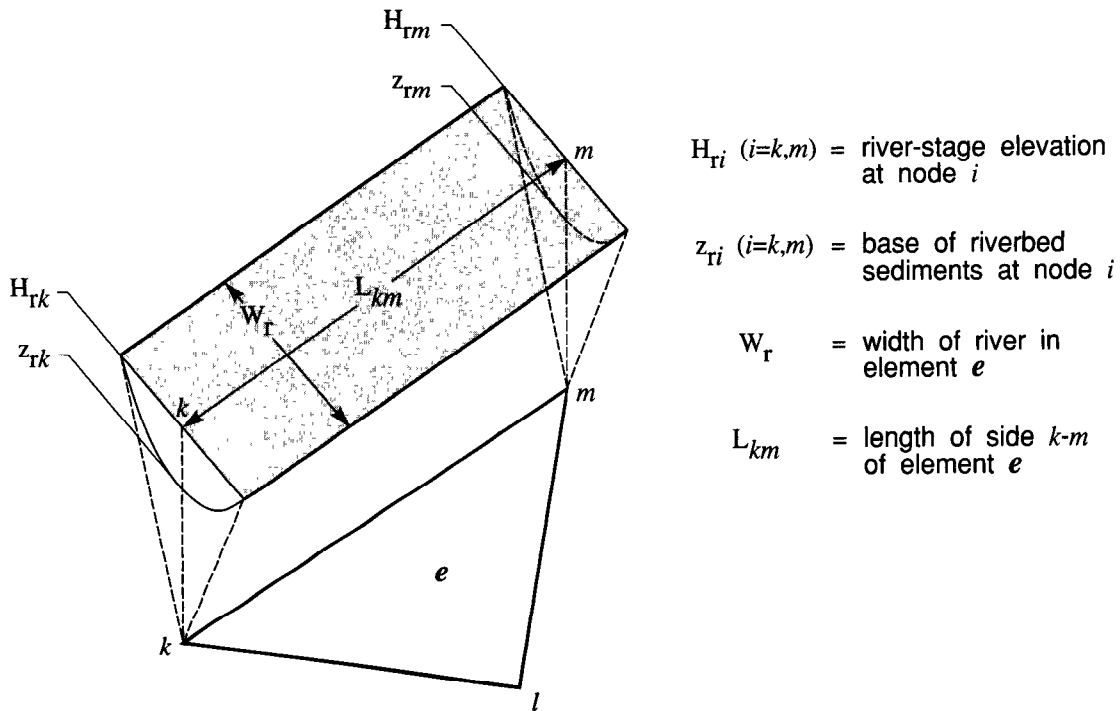
52

Figure 14b. Cross section showing a configuration of the water-table elevation under a river that is idealized as a line or source sink.

where

$$C_{ri} = \frac{1}{2}\Sigma_{j'} \left(\alpha_r L\right)_{ij'},$$ (155)

Q_{ri} is the volumetric discharge at node i [length^3/time] from leakage involving the line sources or sinks, and L_{ij}, is defined the same as for equation (32) (figure 14c).

H_{ri} $(i=k,m)$ = river-stage elevation at node i

z_{ri} $(i=k,m)$ = base of riverbed sediments at node i

W_r = width of river in element e

L_{km} = length of side k-m of element e

Figure 14c. Nomenclature for side k-m of element e that forms a line head-dependent source or sink.

53

Equation (154) is exactly the same as equation (118) expressing areal head-dependent leakage, except that H_{ri} replaces H_{ai}, C_{ri} replaces C_{ai}, and z_{ri} replaces z_{ti}. Therefore, the expressions and the predictor-corrector solution procedure derived for areal, head-dependent leakage apply to the present case as well.

Leakage of water stored elastically in a confining unit (transient leakage)

Equation (1) can be rewritten in a general form that includes leakage to or from a confining unit as follows (Cooley, 1974, p. 3-9):

$$\frac{\partial}{\partial x}\left[T_{xx}\frac{\partial h}{\partial x} + T_{xy}\frac{\partial h}{\partial y}\right] + \frac{\partial}{\partial y}\left[T_{yx}\frac{\partial h}{\partial x} + T_{yy}\frac{\partial h}{\partial y}\right]$$

$$\pm K'_{zz}\frac{\partial h'}{\partial z}\bigg|_{z=z_c} + W + P = S\frac{\partial h}{\partial t} , \qquad (156)$$

where K'_{zz} is the vertical hydraulic conductivity of the confining unit, h' is the head in the confining unit, and z_c is the elevation of the base of the confining unit (if the confining unit overlies the aquifer) or the elevation of the top of the confining unit (if the confining unit underlies the aquifer).

If the confining unit has no elastic storage capacity and flow in the confining unit is almost vertical, then the leakage rate is

$$\pm K'_{zz}\frac{\partial h'}{\partial z}\bigg|_{z=z_c} = R(H-h) , \qquad (157)$$

and equation (1) results. However, if the confining unit has elastic storage capacity, then the leakage rate must be computed using an unsteady-state equation for flow in the confining unit. The formulation of this problem was developed by Hantush (1960), and expanded by Neuman and Witherspoon (1969) and Herrera and his coworkers (Herrera, 1970, 1974; Herrera and Rodarte, 1973; Herrera and Yates, 1977). The following approach is an expansion of their approaches to apply to the finite-element method. For notational simplicity, the confining unit is assumed to overlie the aquifer, because the final function describing leakage to or from the aquifer is the same whether the confining unit overlies or underlies the aquifer. In this case, $z_c = z_t$, the elevation of the base of the confining unit.

Flow in the confining unit is assumed to be almost vertical, which is a reasonable approximation when $K'_{zz}/K_{xx} < 10^{-2}$ (Neuman and Witherspoon, 1969, p. 804). With this assumption, flow in the confining unit at some location (x,y) can be described by the following initial value problem:

$$K'_{zz}\frac{\partial^2 h'}{\partial z^2} = S'_s\frac{\partial h'}{\partial t} \qquad (158)$$

54

subject to

$$h' = h(t), \quad z = z_t, \quad t \geq 0,$$

$$h' = H(t), \quad z = z_t + b', \quad t \geq 0, \tag{159}$$

$$h' = H'_0(z), \quad z_t \leq z \leq z_t + b', \quad t = 0,$$

where S'_s is specific storage of the confining unit [length^{-1}], b' is the

thickness of the confining unit, h is head in the aquifer, H is head at the distal side of the confining unit (assumed to be a known function of time), $H'_0(z)$ is the initial steady-state distribution of head in the confining

unit, $H'_0\left(z_t\right) = h(0)$, and $H'_0\left(z_t + b'\right) = H(0)$.

To initiate development of the leakage function to be inserted into the finite-element equations, spatial finite-element discretization is applied to the general leakage rate in the same manner as it was to $R(H-h)$ to yield

$$\sum_{e_i}\iint_{\Delta^e} \bar{N}^e_i K'_{zz} \left.\frac{\partial h'}{\partial z}\right|_{z=z_t} d\bar{x}d\bar{y} \approx \frac{1}{3e}\sum K'^e_{zz}\Delta^e \left.\frac{\partial h'_i}{\partial z}\right|_{z=z_t}, \tag{160}$$

where, to conform with R, K'_{zz} is assumed to be constant in element e.

Equation (160) expresses the total leakage rate across the patch of elements for node i in terms of the hydraulic gradient at node i. Thus, the equation for flow in the confining unit at node i must yield equation (160) when used to obtain the leakage rate. This flow equation is derived as follows. Integration of equation (158) from z_t to $z \leq z_t + b'$ and solution for the

leakage rate across the base of the confining unit yields

$$K'_{zz}\left.\frac{\partial h'}{\partial z}\right|_{z=z_t} - K'_{zz}\frac{\partial h'}{\partial z} - S'_s\int_{z_t}^{z}\frac{\partial h'}{\partial t}dz, \tag{161}$$

which, when substituted into the integral in equation (160), yields an expression for the approximate leakage across the patch of elements for node i in the form of

$$\frac{1}{3e}\sum_i K'^e_{zz}\Delta^e\left.\frac{\partial h'_i}{\partial z}\right|_{z=z_t} = \frac{1}{3e}\sum_i K'^e_{zz}\Delta^e\frac{\partial h'}{\partial z} - \frac{1}{3e}\sum_i S'^e_s\Delta^e\int_{z_t}^{z}\frac{\partial h'}{\partial t}dz, \tag{162}$$

where S'^e_s is the specific storage of the confining unit in element e.

Differentiation of equation (162) with respect to z yields the equation for flow in the confining unit at node i as

$$\sum_{e_i} K'^e_{zz}\Delta^e\frac{\partial^2 h'_i}{\partial z^2} = \sum_{e_i} S'^e_s\Delta^e\frac{\partial h'_i}{\partial t}. \tag{163}$$

The leakage rate given by equation (160) is calculated using the head in the confining unit, h'_i, which is obtained by analytically solving equation (163). Appropriate boundary and initial conditions are given by $\wedge$ equations (159) written for node i using approximate head in the aquifer h_i in place of exact head h_i. That is,

55

$$h_i' = \hat{h}_i(t), \quad z = z_{ti}, \quad t \geq 0,$$

$$h_i' = H_i(t), \quad z = z_{ti} + b_i', \quad t \geq 0, \tag{164}$$

$$h_i' = H_{0i}'(z), \quad z_{ti} \leq z \leq z_{ti} + b_i', \quad t = 0,$$

where b_i' is a weighted average thickness of the confining unit for all

elements in the patch for node i that is derived further on. The solution to this initial value problem was obtained by Carslaw and Jaeger (1959, p. 102-104) and can be written in the form

$$h_i'(z,t) = 2 \sum_{m=1}^{\infty} \frac{1}{m\pi} \sin \frac{m\pi \left[z - z_t\right]}{b_i'} \int_0^t \frac{d\eta_{mi}(\tau)}{d\tau} e^{-(m\pi)^2 \gamma_i (t-\tau)} d\tau$$

$$+ \frac{H_i(t) - \hat{h}_i(t)}{b_i'} \left(z - z_{ti}\right) + \hat{h}_i(t), \tag{165}$$

where

$$\eta_{mi}(t) = (-1)^m H_i(t) - \hat{h}_i(t) \tag{166}$$

and

$$\gamma_i = \frac{\sum_{e_i} K'^e_{zz} \Delta^e}{b_i'^2 \sum_{e_i} S'^e_s \Delta^e}. \tag{167}$$

The leakage rate at time t, $K'_{zz} \partial h_i' / \partial z \big|_{z=z_t}$, is computed from equations

(165) and (166). When this is substituted into equation (160), the leakage rate across the patch of elements for node i is obtained as

$$\frac{1}{3} \sum_{e_i} K'^e_{zz} \Delta^e \frac{\partial h_i'}{\partial z} \bigg|_{z=z_t} = \frac{2}{3b_i'} \sum_{e_i} K'^e_{zz} \Delta^e \sum_{m=1}^{\infty} (-1)^m \int_0^t \frac{dH_i(\tau)}{d\tau} e^{-(m\pi)^2 \gamma_i (t-\tau)} d\tau$$

$$- \frac{2}{3b_i'} \sum_{e_i} K'^e_{zz} \Delta^e \sum_{m=1}^{\infty} \int_0^t \frac{d\hat{h}_i(\tau)}{d\tau} e^{-(m\pi)^2 \gamma_i (t-\tau)} d\tau$$

$$+ \frac{1}{3b_i'} \sum_{e_i} K'^e_{zz} \Delta^e \left[H_i(t) - \hat{h}_i(t)\right]. \tag{168}$$

As $S'^e_s \to 0$, equation (168) should approach the leakage term based on equation (27). That is,

$$\frac{1}{3b'_i} \sum_e \sum_i K'^e_{zz} \Delta^e \left(H_i - \hat{h}_i \right) = \frac{1}{3} \sum_e \sum_i R^e \Delta^e \left(H_i - \hat{h}_i \right). \tag{169}$$

Therefore, the weighted average thickness b'_i should be defined by

$$b'_i = \frac{\sum_e \sum_i K'^e_{zz} \Delta^e}{\sum_e \sum_i R^e \Delta^e} \tag{170}$$

to make equations (168) and (27) consistent. Because R^e is K'^e_{zz} divided by the confining-unit thickness for element e, b'_i is a weighted harmonic mean of confining-unit thicknesses.

The leakage functions to be inserted into the finite-element equations are developed from equation (168). To yield a useful form for the leakage functions, the integrals must be evaluated and the infinite series must be approximated. The integrals can be approximated by using the procedure of Cooley (1972), in which the integrals for time level $t = t_{n+1}$ are evaluated in terms of integrals for time level $t = t_n$, which have already been evaluated. Thus, the necessity for storing the heads for all previous time levels is avoided. The procedure is applied to the second integral in equation (168), for example, as follows:

$$\int_0^{t_{n+1}} \frac{d\hat{h}_i(\tau)}{d\tau} e^{-(m\pi)^2 \gamma_i \left(t_{n+1} - \tau \right)} d\tau$$

$$= \int_0^{t_n} \frac{d\hat{h}_i(\tau)}{d\tau} e^{-(m\pi)^2 \gamma_i \left(t_n + \Delta t_{n+1} - \tau \right)} d\tau + \int_{t_n}^{t_{n+1}} \frac{d\hat{h}_i(\tau)}{d\tau} e^{-(m\pi)^2 \gamma_i \left(t_{n+1} - \tau \right)} d\tau$$

$$= e^{-(m\pi)^2 \gamma_i \Delta t_{n+1}} \int_0^{t_n} \frac{d\hat{h}_i(\tau)}{d\tau} e^{-(m\pi)^2 \gamma_i \left(t_n - \tau \right)} d\tau$$

$$+ \frac{\hat{h}_{i,n+1} - \hat{h}_{i,n}}{\Delta t_{n+1}} \int_{t_n}^{t_{n+1}} e^{-(m\pi)^2 \gamma_i \left(t_{n+1} - \tau\right)} d\tau$$

$$= e^{-(m\pi)^2 \gamma_i \Delta t_{n+1}} \int_0^{t_n} \frac{d\hat{h}_i(\tau)}{d\tau} e^{-(m\pi)^2 \gamma_i \left(t_n - \tau\right)} d\tau$$

$$+ \frac{\hat{h}_{i,n+1} - \hat{h}_{i,n}}{\Delta t_{n+1}} \frac{1}{(m\pi^2)\gamma_i} \left[1 - e^{-(m\pi)^2 \gamma_i \Delta t_{n+1}}\right]. \tag{171}$$

By multiplying equation (171) by 2 (for convenience in later manipulations) and defining

$$I_{mi,n} = 2 \int_0^{t_n} \frac{d\hat{h}_i(\tau)}{d\tau} e^{-(m\pi)^2 \gamma_i \left(t_n - \tau\right)} d\tau, \tag{172}$$

a recursive relation for evaluating the integral is obtained as

$$I_{mi,n+1} = e^{-(m\pi)^2 \gamma_i \Delta t_{n+1}} I_{mi,n} + \frac{\hat{h}_{i,n+1} - \hat{h}_{i,n}}{\Delta t_{n+1}} \frac{2}{(m\pi)^2 \gamma_i} \left[1 - e^{-(m\pi)^2 \gamma_i \Delta t_{n+1}}\right], \tag{173}$$

where $I_{mi,0} = 0$. Equation (173) permits evaluation of $I_{mi,n+1}$ from $I_{mi,n}$ and the heads at only the current (n+1) and previous (n) time levels. In an analogous manner, $2(-1)^m$ times the first integral in equation (168) is evaluated as

$$J_{mi,n+1} = e^{-(m\pi)^2 \gamma_i \Delta t_{n+1}} J_{mi,n}$$

$$+ \frac{H_{i,n+1} - H_{i,n}}{\Delta t_{n+1}} \frac{2(-1)^m}{(m\pi)^2 \gamma_i} \left[1 - e^{-(m\pi)^2 \gamma_i \Delta t_{n+1}}\right], \tag{174}$$

where

$$J_{mi,n} = 2(-1)^m \int_0^{t_n} \frac{dH_i(\tau)}{d\tau} e^{-(m\pi)^2 \gamma_i \left(t_n - \tau\right)} d\tau. \tag{175}$$

Next, the infinite series in equation (168) are approximated by finite series so that a large number of terms given by equations (172) through (175) do not have to be computed and saved at each time level. The

58

coefficients of the finite series are determined so that a small number of terms of the finite series can be used to give a good approximation of results obtained with the infinite series. The approximations are

$$2\sum_{m=1}^{\infty}\int_{0}^{t_{n+1}}\frac{d\hat{h}_i(\tau)}{d\tau}\,e^{-(m\pi)^2\gamma_i\left(t_{n+1}-\tau\right)}\,d\tau \simeq \sum_{m=1}^{N_1} A'_m\int_{0}^{t_{n+1}}\frac{d\hat{h}_i(\tau)}{d\tau}\,e^{-\alpha_m\gamma_i\left(t_{n+1}-\tau\right)}\,d\tau \quad (176)$$

and

$$2\sum_{m=1}^{\infty}(-1)^m\int_{0}^{t_{n+1}}\frac{dH_i(\tau)}{d\tau}\,e^{-(m\pi)^2\gamma_i\left(t_{n+1}-\tau\right)}\,dt \simeq \sum_{m=1}^{N_2} B'_m\int_{0}^{t_{n+1}}\frac{dH_i(\tau)}{d\tau}\,e^{-\beta_m\gamma_i\left(t_{n+1}-\tau\right)}\,d\tau, \quad (177)$$

where A'_m, α_m, B'_m, and β_m are coefficients to be determined, and N_1 and N_2 are the numbers of terms in the two finite series.

By repeating the derivation leading to equation (171) using the approximations, it can be seen that equations (173) and (175) are approximated by

$$\hat{I}_{mi,n+1} = e^{-\alpha_m\gamma_i\Delta t_{n+1}}\hat{I}_{mi,n} + \frac{\hat{h}_{i,n+1} - \hat{h}_{i,n}}{\Delta t_{n+1}}\frac{A'_m}{\alpha_m\gamma_i}\left(1-e^{-\alpha_m\gamma_i\Delta t_{n+1}}\right), \quad (178)$$

where

$$\hat{I}_{mi,n} = A'_m\int_{0}^{t_n}\frac{d\hat{h}_i(\tau)}{d\tau}\,e^{-\alpha_m\gamma_i\left(t_n-\tau\right)}\,d\tau, \quad (179)$$

and

$$\hat{J}_{mi,n+1} = e^{-\beta_m\gamma_i\Delta t_{n+1}}\hat{J}_{mi,n} + \frac{H_{i,n+1} - H_{i,n}}{\Delta t_{n+1}}\frac{B'_m}{\beta_m\gamma_i}\left(1 - e^{-\beta_m\gamma_i\Delta t_{n+1}}\right), \quad (180)$$

where

$$\hat{J}_{mi,n} = B'_m\int_{0}^{t_n}\frac{dH_i(\tau)}{d\tau}\,e^{-\beta_m\gamma_i\left(t_n-\tau\right)}\,d\tau. \quad (181)$$

The leakage rate computed using equations (178) and (180) is approximately equal to the exact leakage rate computed using equations (173) and (174) if

$$2\sum_{m=1}^{\infty}\frac{1}{(m\pi)^2}\left(1 - e^{-(m\pi)^2\gamma_i\Delta t_{n+1}}\right) \simeq \sum_{m=1}^{N_1}\frac{A'_m}{\alpha_m}\left(1 - e^{-\alpha_m\gamma_i\Delta t_{n+1}}\right), \quad (182)$$

and

$$2\sum_{m=1}^{\infty}\frac{(-1)^m}{(m\pi)^2}\left(1 - e^{-(m\pi)^2\gamma_i\Delta t_{n+1}}\right) \simeq \sum_{m=1}^{N_2}\frac{B'_m}{\beta_m}\left(1 - e^{-\beta_m\gamma_i\Delta t_{n+1}}\right). \quad (183)$$

To obtain the best approximations, equations (182) and (183) should hold exactly when $\Delta t_{n+1} = 0$ and when $\Delta t_{n+1} \to \infty$. The first requirement helps

59

yield an accurate solution for small time elements and is automatically fulfilled because both pairs of series equal zero when $\Delta t_{n+1} = 0$. The second requirement ensures that the total yield from storage in the confining unit under a unit head change that is fixed indefinitely is preserved by the approximation (Herrera and Yates, 1977, p. 726-727). Herrera and Yates (1977, p. 727) found the accuracy of their approximate solutions to be highly sensitive to fulfillment of this requirement. By letting $\Delta t_{n+1} \rightarrow \infty$ in equations (182) and (183) and using the sums of the resulting infinite series (Herrera and Yates, 1977, p. 727), it can be seen that this requirement is fulfilled if

$$2 \sum_{m=1}^{\infty} \frac{1}{(m\pi)^2} = \frac{1}{3} = \sum_{m=1}^{N_1} \frac{A'_m}{\alpha_m} \tag{184}$$

and

$$2 \sum_{m=1}^{\infty} \frac{(-1)^m}{(m\pi)^2} = -\frac{1}{6} = \sum_{m=1}^{N_2} \frac{B'_m}{\beta_m}. \tag{185}$$

It remains to find coefficients A'_m, α_m, B'_m, and β_m so that approximations given by equations (182) and (183) are good with a small number of terms, N_1 and N_2. For notational convenience, dimensionless time element Δt_D is defined by $\Delta t_D = \gamma_i \Delta t_n$, and the series are denoted as

$$S_1\left(\Delta t_D\right) = 2 \sum_{m=1}^{\infty} \frac{1}{(m\pi)^2} \left[1 - e^{-(m\pi)^2 \Delta t_D}\right], \tag{186}$$

$$S_2\left(\Delta t_D\right) = 2 \sum_{m=1}^{\infty} \frac{(-1)^m}{(m\pi)^2} \left[1 - e^{-(m\pi)^2 \Delta t_D}\right], \tag{187}$$

$$M_1\left(\Delta t_D\right) = \sum_{m=1}^{N_1} A_m \left[1 - e^{-\alpha_m \Delta t_D}\right], \tag{188}$$

and

$$M_2\left(\Delta t_D\right) = \sum_{m=1}^{N_2} B_m \left[1 - e^{-\beta_m \Delta t_D}\right], \tag{189}$$

where

$$A_m = \frac{A'_m}{\alpha_m} \tag{190}$$

and

$$B_m = \frac{B'_m}{\beta_m}. \tag{191}$$

Because both sets of series are functions of only Δt_D, the coefficients A_m, B_m, α_m, and β_m can be uniquely obtained by fitting approximate, finite series $M_1\left(\Delta t_D\right)$ and $M_2\left(\Delta t_D\right)$ to infinite series $S_1\left(\Delta t_D\right)$ and $S_2\left(\Delta t_D\right)$, respectively, using a range of values for Δt_D sufficient to include most time-element sizes and values of γ_i.

The coefficients were determined using nonlinear least squares (see Cooley and Naff, 1990, p. 61-64) applied to the weighted sum of squared error functions

$$SS_1 = \sum_{n=1}^{P_t} \frac{\left[S_1\left(\Delta t_D\right) - M_1\left(\Delta t_D\right)\right]^2}{\left|S_1(\Delta t_D)\right|} \tag{192}$$

and

$$SS_2 = \sum_{n=1}^{P_t} \frac{\left[S_2\left(\Delta t_D\right) - M_2\left(\Delta t_D\right)\right]^2}{\left|S_2\left(\Delta t_D\right)\right|} \tag{193}$$

subject to the constraints given by equations (184) and (185). The number of dimensionless times used in the fitting process, P_t, was set equal to 25, and $\Delta t_D = 1 \times 10^{-6}$, 2.5×10^{-6}, 5×10^{-6}, 1×10^{-5}, 2.5×10^{-5}, $5 \times 10^{-5}, \ldots, 1 \times 10^2$. The weights $1/\left|S_1\left(\Delta t_D\right)\right|$ and $1/\left|S_2\left(\Delta t_D\right)\right|$ are somewhat arbitrary, but were found to give good approximations for both small and large dimensionless time elements. Constraints were applied by specifying

$$A_{N_1} = \frac{1}{3} - \sum_{m=1}^{N_1-1} A_m \tag{194}$$

and

$$B_{N_2} = -\frac{1}{6} - \sum_{m=1}^{N_2-1} B_m. \tag{195}$$

Thus, the coefficients determined by nonlinear least squares are N_1 values of α_m and N_1-1 values of A_m for equation (192) and N_2 values of β_m and N_2-1 values of B_m for equation (193).

Good fits for both least squares problems were obtained with $N_1 = 3$ and $N_2 = 2$, and the resulting approximations are illustrated in figures 15 and 16. Values of the coefficients determined are

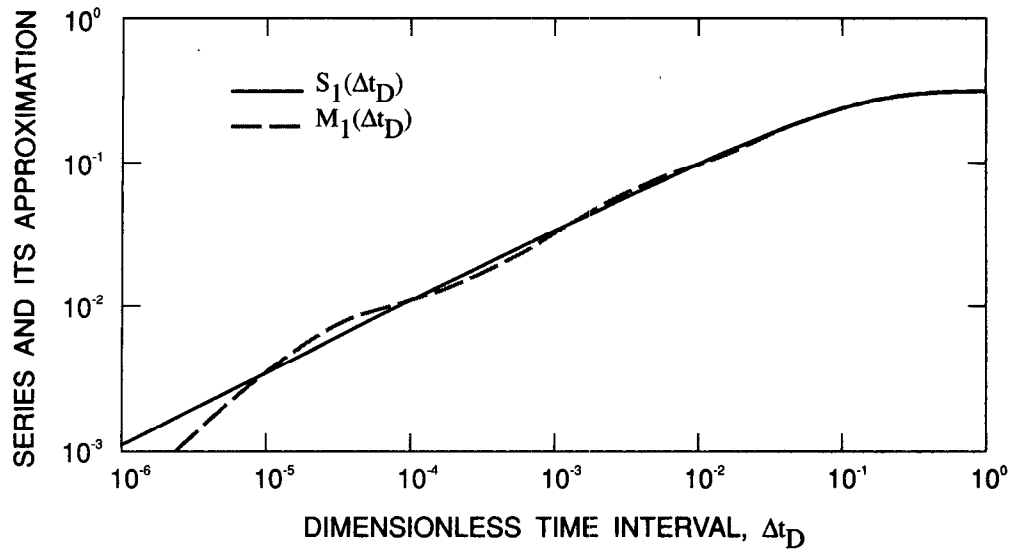|	
$A_1 = 0.26484$,	$\alpha_3 = 49538$,
$A_2 = 0.060019$,	$B_1 = -0.25754$,
$A_3 = 0.0084740$,	$B_2 = 0.090873$,
$\alpha_1 = 13.656$,	$\beta_1 = 10.764$,
$\alpha_2 = 436.53$,	$\beta_2 = 19.805$.

61

Figure 15. Relationship between series $S_1(\Delta t_D)$ defined by equation (186) and its approximation $M_1(\Delta t_D)$ defined by equation (188).
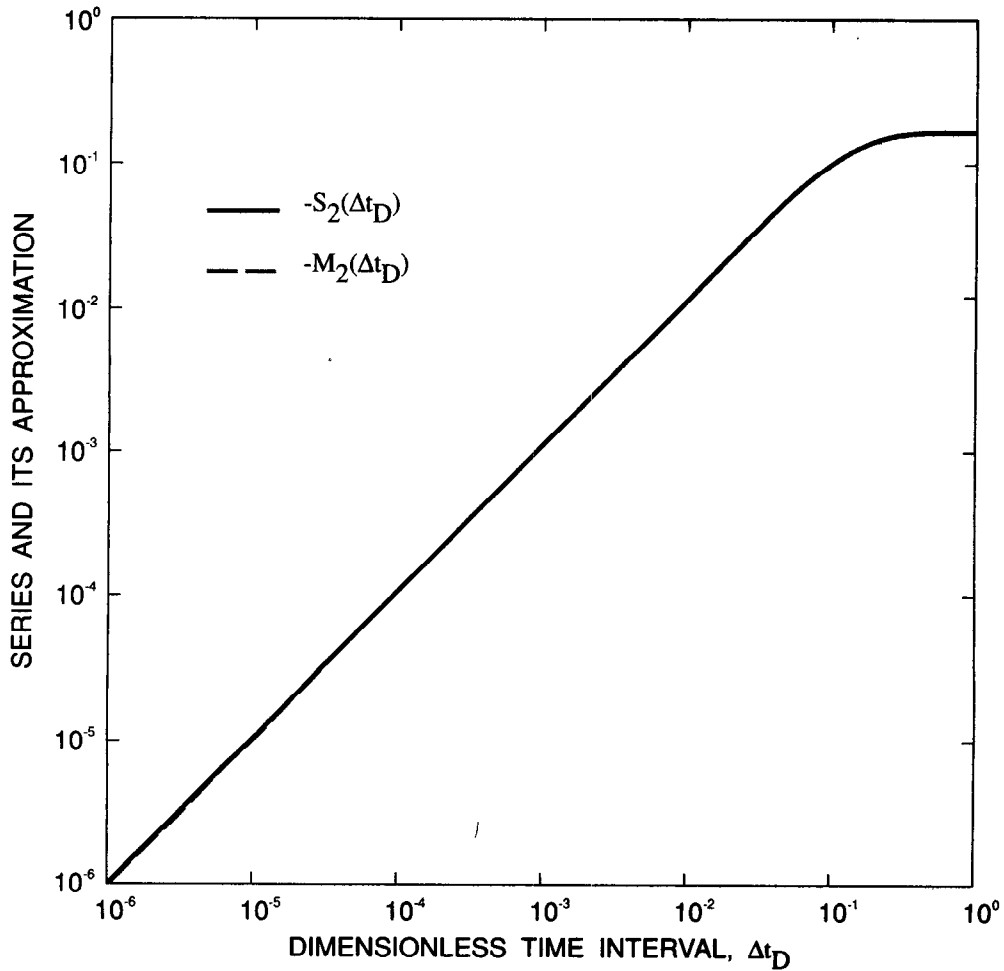

Figure 16. Relationship between series $-S_2(\Delta t_D)$ defined by equation (187) and its approximation $-M_2(\Delta t_D)$ defined by equation (189).

The final step leading to the leakage function to incorporate into the finite-element equations is to integrate the product of equation (168) and σ_{n+1} over time element n+1 by assuming that $\partial h_i'/\partial z\big|_{z=z_t}$ varies linearly like $\hat{h}_i$ (which is consistent with the treatment of R(H - h)). Therefore (see equation (54)),

$$\left(\frac{1}{3}\sum_{e_i} K_{zz}'^e\Delta^e\right)\int_0^{\Delta t_{n+1}} \frac{\partial h_i'}{\partial z}\bigg|_{z=z_t}\sigma_{n+1}\,dt'$$

$$= \frac{1}{6}\Delta t_{n+1}\left(\frac{1}{3}\sum_{e_i} K_{zz}'^e\Delta^e\right)\left(\frac{\partial h_{i,n}'}{\partial z} + 2\frac{\partial h_{i,n+1}'}{\partial z}\right)_{z=z_t} \tag{196}$$

By using equations (168), (170), and (176) through (181), the leakage rates at time levels n and n+1 in equation (196) are evaluated as, respectively,

$$\left(\frac{1}{3}\sum_{e_i} K_{zz}'^e\Delta^e\right)\frac{\partial h_{i,n}'}{\partial z}\bigg|_{z=z_t} \simeq \left(\frac{1}{3}\sum_{e_i} R^e\Delta^e\right)\left[\sum_{m=1}^{N_2}\hat{J}_{mi,n} - \sum_{m=1}^{N_1}\hat{I}_{mi,n} + H_{i,n} - \hat{h}_{i,n}\right] \tag{197}$$

and

$$\left(\frac{1}{3}\sum_{e_i} K_{zz}'^e\Delta^e\right)\frac{\partial h_{i,n+1}'}{\partial z}\bigg|_{z=z_t} \simeq \left(\frac{1}{3}\sum_{e_i} R^e\Delta^e\right)\left[\sum_{m=1}^{N_2} e^{-\beta_m\gamma_i\Delta t_{n+1}}\hat{J}_{mi,n}\right.$$

$$+ \frac{H_{i,n+1} - H_{i,n}}{\Delta t_{n+1}\gamma_i} M_2\left(\gamma_i\Delta t_{n+1}\right)$$

$$- \sum_{m=1}^{N_1} e^{-\alpha_m\gamma_i\Delta t_{n+1}}\hat{I}_{mi,n} - \frac{\hat{h}_{i,n+1} - \hat{h}_{i,n}}{\Delta t_{n+1}\gamma_i} M_1\left(\gamma_i\Delta t_{n+1}\right) + H_{i,n+1} - \hat{h}_{i,n+1}\right] \tag{198}$$

To obtain the leakage function to incorporate into the finite-element equations, equation (196) is multiplied by $-2/\Delta t_{n+1}$ and equations (197) and (198) are substituted into it. For notational compactness of the resulting expression, the following quantities are defined.

$$P_{hi,n} = \left(\frac{1}{3}\sum_{e_i} R^e\Delta^e\right)\sum_{m=1}^{N_1}\hat{I}_{mi,n}, \tag{199}$$

$$P_{Hi,n} = \left(\frac{1}{3}\sum_{e_i} R^e\Delta^e\right)\sum_{m=1}^{N_2}\hat{J}_{mi,n}, \tag{200}$$

$$Q_{hi,n} = \left(\frac{1}{3}\sum_{e_i} R^e\Delta^e\right)\sum_{m=1}^{N_1} e^{-\alpha_m\gamma_i\Delta t_{n+1}}\hat{I}_{mi,n}, \tag{201}$$

$$Q_{Hi,n} = \left[\frac{1}{3}\sum_e R^e \Delta^e\right] \sum_{m=1}^{N_2} e^{-\beta_m \gamma_i \Delta t_{n+1}} \hat{J}_{mi,n}, \qquad (202)$$

$$C_{hi,n+1} = \left[\frac{1}{3}\sum_e R^e \Delta^e\right] \frac{M_1\left[\gamma_i \Delta t_{n+1}\right]}{\gamma_i}, \qquad (203)$$

$$C_{Hi,n+1} = \left[\frac{1}{3}\sum_e R^e \Delta^e\right] \frac{M_2\left[\gamma_i \Delta t_{n+1}\right]}{\gamma_i}, \qquad (204)$$

$$C_{Ri} = \frac{1}{3}\sum_e R^e \Delta^e. \qquad (205)$$

Therefore, the final leakage function is

$$-\frac{1}{3}\left(P_{Hi,n} + 2Q_{Hi,n}\right) - \frac{2}{3}C_{Hi,n+1}\frac{H_{i,n+1} - H_{i,n}}{\Delta t_{n+1}} + \frac{1}{3}\left(P_{hi,n} + 2Q_{hi,n}\right)$$

$$+\frac{2}{3}C_{hi,n+1}\frac{\hat{h}_{i,n+1} - \hat{h}_{i,n}}{\Delta t_{n+1}} - C_{Ri}\left[\frac{1}{3}\left(H_{i,n} - \hat{h}_{i,n}\right) + \frac{2}{3}\left(H_{i,n+1} - \hat{h}_{i,n+1}\right)\right]$$

$$= \left[\frac{C_{hi,n+1}}{\Delta t_{n+1}} + C_{Ri}\right]\delta_i - \frac{1}{3}\left(P_{Hi,n} + 2Q_{Hi,n}\right) - \frac{2}{3}C_{Hi,n+1}\frac{H_{i,n+1} - H_{i,n}}{\Delta t_{n+1}}$$

$$+\frac{1}{3}\left(P_{hi,n} + 2Q_{hi,n}\right) - \frac{1}{3}C_{Ri}\left[H_{i,n} - \hat{h}_{i,n} + 2\left(H_{i,n+1} - \hat{h}_{i,n}\right)\right] \qquad (206)$$

The leakage process described by equation (206) is time dependent, but linear. Therefore, equation (206) is added into equation (58), unless the predictor-corrector method is required to include other phenomena, in which case equation (206) is added into the appropriate predictor and corrector equations. The coefficient of δ_i is added into $\underline{V}$ for every node i where

leakage occurs, and the remaining terms are subtracted from the right-hand side.

FINITE-ELEMENT FORMULATION IN AXISYMMETRIC CYLINDRICAL COORDINATES

GOVERNING FLOW EQUATION AND BOUNDARY CONDITIONS

Axially symmetric ground-water flow in an aquifer is assumed to be governed by the following unsteady-state flow equation written in axisymmetric cylindrical coordinates (Bear, 1979, p. 116):

$$\frac{1}{r}\frac{1}{\partial r}\left(K_{rr}r\frac{\partial h}{\partial r}\right) + \frac{\partial}{\partial z}\left(K_{zz}\frac{\partial h}{\partial z}\right) = S_s\frac{\partial h}{\partial t}, \qquad (207)$$

64